Supporting Information for

Phase separation modulates the thermodynamics and kinetics of RNA hybridization

Atul K. Rangadurai[†‡¡⊥*], Lisa Ruetz[∃], Rashik Ahmed[†‡¡⊥], Kristen Lo[¡], Martin Tollinger[∃], Julie D. Forman-Kay[¡,⊥], Christoph Kreutz[∃], Lewis E. Kay[†‡¡⊥*]

[†]Department of Molecular Genetics, University of Toronto, Toronto, ON, M5S 1A8, Canada

[‡]Department of Chemistry, University of Toronto, Toronto, ON, M5S 3H6, Canada

[¡]Department of Biochemistry, University of Toronto, Toronto, ON, M5S 1A8, Canada

[⊥]Program in Molecular Medicine, Hospital for Sick Children Research Institute, Toronto, ON, M5G 0A4, Canada

[∃]Institute of Organic Chemistry and Center for Molecular Biosciences Innsbruck (CMBI), University of Innsbruck, Innrain 80/82, 6020 Innsbruck, Austria

This PDF file includes:

Supporting Information Text

Materials and Methods

Sample preparation

The N623TN630T double mutant of the C-terminal region of CAPRIN1 (residues 607-709, Uniprot ID Q14444) was expressed and purified as described previously[1-2]. The final size exclusion chromatography purification step using a Superdex 75 26/600 column was carried out under RNAse free conditions by passing RNaseOUT solution (G-Biosciences Catalog No. 786-71) through the FPLC system and column, prior to equilibration with buffer (50mM Tris, 200mM NaCl, 3M guanidinium hydrochloride, pH 8.0). The 96-well fraction collector plates used for collecting fractions were also dry autoclaved after rinsing with diethylpyrocarbonate (DEPC) water prior to usage. Fractions containing purified protein (as confirmed by SDS-PAGE) were pooled together and exchanged into NMR buffer (10mM sodium phosphate, pH 7.0, 10% D_2O) by passing four times through a 3kDa Amicon centrifugal concentrator (Millipore Sigma, Catalog No. UFC9003). The pH of the concentrated protein (~10mM) solution was adjusted to 7.0 by the addition of concentrated HCl using a micro pH electrode.

The unlabeled RNA single strand (5'-GCCAAUCGAUGC-3') used in this study (Figure 1A) was purchased from IDT with standard desalting purification. The 5'-GCAUC**G**AUUGGC-3' (Figure 1A) and 5'-GCCAA**U**CGAUGC-3' (Figures S1A and S2A) RNA single strands, with the G/U residue in bold denoting 2'-O-$^{13}CH_3$ labeling, were synthesized using phosphoramidite chemistry[3-4] on an ABI 391 PCR-MATE (Applied Biosystems) utilizing a self-written synthetic cycle. Standard 2'-O-TBDMS RNA phosphoramidites (rA^{Ac}, rC^{Ac}, rG^{Ac} and rU, *Chemgenes*, USA), in-house synthesized 2'-O$^{13}CH_3$-U[3] and 2'-O$^{13}CH_3$-G RNA phosphoramidites, and controlled pore glass (CPG) RNA solid support (1000 Å pore size, ChemeGenes, USA) with an average loading of 40 μmol g^{-1}, were used. During the solid phase synthesis, the following solutions were used: *Cap A*: acetic anhydride/lutidine/tetrahydrofuran 1/1/8, v/v/v; *Cap B*: tetrahydrofuran/N-methylimidazole 86/16 v/v; *Oxidation solution*: 500 mg iodine dissolved in a mixture of 70 mL tetrahydrofuran, 20 mL pyridine, and 10 mL water; *Detritylation solution*: 4% dichloroacetic acid in anhydrous toluene. The amidite (0.1 M) and S-benzylthiotetrazole (0.25M, coupling) solutions were dried using activated molecular sieves (3 Å) for at least 48 hours before usage.

Alkaline deprotection was performed by adding 1 mL aqueous methylamine (40%) and 1 mL aqueous ammonia (28%) to the solid support. The reaction tube was incubated at 37 °C for 5 hours. The solid support was filtered off and washed three times with H_2O/ tetrahydrofuran (1.0 mL; 1/1, v/v). The combined liquid phases were evaporated to dryness and dried under high vacuum for 1 hour. 2'-O-TBDMS deprotection was

performed by dissolving the residue in 300 µL anhydrous dimethylsulfoxide, adding 375 µL triethylamine trihydrofluoride, and incubating the reaction tube at 37 °C for 16 hours. The reaction mixture was quenched with 2 mL quenching buffer (*GlenResearch*, USA) and the solution applied to a HiPrep 26/10 desalting column (*GE Healthcare*, Austria) using a ÄKTA start system (*GE Healthcare*, Austria). The crude RNA was eluted using HPLC grade water, the RNA containing fractions collected in a 50 mL round bottom flask and the water evaporated. The crude RNA was dissolved in 1 mL HPLC grade H_2O and transferred to a 1.5 mL reaction tube.

The crude RNA was applied to a Dionex DNAPac® PA-100 column (4 mm x 250 mm) at 80 °C with a flow rate of 10 mL/min for purification. A gradient of 10–30% B in 40 min was applied; Eluent A: 20 mM $NaClO_4$, 25 mM Tris·HCl, pH 8.0, 20% v/v acetonitrile; Eluent B: 600 mM $NaClO_4$, 25 mM Tris·HCl, pH 8.0, 20% v/v acetonitrile. The fractions containing RNA were combined, the acetonitile evaporated and the remaining solution loaded on a C18 SepPak catridge (*Waters*, Austria) to remove HPLC buffer salts. The purified RNA was eluted from the C18 column using water/acetonitrile (1/1, v/v), the solvents evaporated, and the residue dissolved in HPLC grade H_2O for concentration and mass spectrometry analysis, and lyophilized for storage. The mass of the synthesized oligos (Figure S1) were verified using ion pair reversed phase LC-ESI-MS analysis on a Finnigan LCQ Advantage Max mass spectrometer equipped with an electrospray ionization (ESI) interface coupled to a Thermo Scientific Dionex Ultimate 3000 HPLC system. The sample was applied to a Thermo Scientific DNAPacTM RP column (2.1 x 50 mm) and eluted using an increasing gradient from Buffer A: 8.6 mM triethylamine 100 mM hexafluoriisopropanol in ddH_2O (MilliQ) to Buffer B: MeOH.

The RNA single strands were dissolved in Milli Q water and their concentrations estimated using extinction coefficients obtained from the ADT Bio Oligo Calculator (https://atdbio.com/tools/oligo-calculator), assuming that the 2'-O-$^{13}CH_3$ modification does not affect the extinction coefficient. The two single strands were mixed in equimolar amounts and annealed by heating to 95 °C for 5 minutes and cooling down at room temperature, at a concentration of ~500 µM. The annealed duplex was exchanged into NMR buffer (10mM sodium phosphate, pH 7.0, 10% D_2O) by passing four times through a 3kDa Amicon centrifugal concentrator and concentrated down to ~1.3mM.

Based on reference values in Basanta Sanchez *et al.*[5], 2'-OCH_3 modified uridine/guanidine has an extinction coefficient that is ~15% smaller than that of its unmodified counterpart. Thus, by making the assumption that the methyl group does not affect the extinction coefficient, we would likely under-estimate the true concentration of the methylated single strand, potentially giving excess unpaired methylated single strands in our duplex preparations (see above). However, we did not observe peaks corresponding to ssRNA in NMR spectra of the RNA duplex of Figure 1A at low

temperatures (25 °C) where it does not have detectable melting (melting temperature of ~70 °C under the conditions of our experiments, 200mM NaCl).

In order to generate the CAPRIN1/RNA phase-separated sample with 2'-O-methyl labeling at G (Figure 1A), concentrated CAPRIN1 (730 μL, 10.2 mM), with annealed duplex comprising singly labeled and unlabeled RNA strands (187 μL, 1.33 mM; see above) were added together in an eppendorf tube on ice, followed by addition of 48.2 μL of buffer containing salt (10 mM sodium phosphate, pH 7.0, 10% D_2O, 4M NaCl) to facilitate formation of the condensed phase. The condensed phase with double labeled RNA (Figure S2A), was prepared in an analogous manner with volumes of each of the solutions smaller by ~4%. The bulk concentrations of salt, CAPRIN1 and RNA were 200 mM, 7.7 mM and 257 μM, respectively. The eppendorf tube was vortexed and then spun down for a few minutes in a centrifuge at 4 °C at 1503g, in order for the condensed phase droplets to coalesce, resulting in the formation of a large macroscopic droplet at the bottom of the eppendorf tube. The condensed phase droplet along with dilute phase at the top was transferred to a 3 mm NMR tube using a syringe.

Care was taken to rinse all glassware used for buffer preparation and storage of RNA samples with RNaseOUT solution and MilliQ water, prior to use. All buffers used for the RNA samples were also prepared with MilliQ water. It should be noted that the MilliQ unit should be equipped with a Biopak polisher (Millipore Sigma, Catalog No. CDUFBI0A1), which is certified to give nuclease free water.

NMR Experiments

All NMR measurements were performed at 23.5 Tesla (1 GHz ^{1}H frequency) on a Bruker Avance Neo spectrometer or at 18.8 Tesla (800 MHz ^{1}H frequency) on a Bruker Avance III HD spectrometer, equipped with cryogenically cooled *x*,*y*,*z* pulsed-field gradient triple-resonance probes. All NMR experiments were processed using the *NMRPipe* suite of programs[6]. Peak volumes in ddHMQC spectra[7-8] for the measurement of populations of dsRNA/ssRNA (Figure 1D) and in ddHSQC-based magnetization exchange spectra (Figure S5A) to measure the kinetics of dsRNA/ssRNA interconversion (Figures 2B and 2C, Figure S7) were analyzed using *NMRPipe*, while datasets quantifying effective ^{1}H relaxation rates (Figure S5B) and RNA diffusion (Figure 1E) were analyzed using *peakipy* (https://j-brady.github.io/peakipy/). The pulse sequences for measurement of magnetization exchange and effective ^{1}H relaxation rates (Figure S5) are provided in Supporting Information and posted along with parameters to Zenodo (https://doi.org/10.5281/zenodo.11132297), along with processing scripts for analysis of the magnetization exchange experiments.

Pulse field gradient diffusion NMR experiments for measuring diffusion coefficients of ssRNA in buffer (25 μM sample; Figure 1E, gray, 200 mM NaCl), using the 2'-O-$^{13}CH_3$ probe, were performed using a single quantum (SQ) experiment recorded in a 1D manner, as described previously[9], except that ^{15}N and ^{13}C channels were interchanged. A pair of bipolar gradients was used for dephasing and rephasing[10], with total durations of each bipolar pair (δ) and diffusion time (Δ) of (1414.2 μs and 100 ms) or (1000 μs and 200 ms); similar values of the diffusion coefficient (*D,* see below) were obtained in both cases, indicating that convection is not an issue in the measurements. Diffusion data for the methyl group of ssRNA in the condensed phase (Figure 1E, green) were obtained using a SQ experiment recorded in a 2D manner, with gradients for coherence selection to eliminate t_1 noise from residual signals derived from CAPRIN1, with δ = 3590 μs and Δ = 400 ms. It should be noted that the signal for the dsRNA species could not be observed in these diffusion measurements due to its fast relaxation. The diffusion coefficient for CAPRIN1 in the condensed phase (Figure 1E, blue) was obtained using a triple quantum (TQ) experiment[11] recorded in a 1D manner, with coherence transfer selection gradients and values of δ and Δ = (2000 μs, 400 ms) or (3000 μs and 177.7 ms). As for ssRNA in buffer, similar values of the diffusion coefficient (*D*) were obtained in both cases, indicating the absence of contributions from convection. All diffusion experiments were recorded at 57.5 °C at 800 MHz (maximum gradient strength of 44.6 G/cm).

The fractional water content of the RNA:CAPRIN1 condensate of Figure 1 relative to RNA in buffer (100 μM RNA in 10 mM sodium phosphate, 10% D_2O, pH 7.0, 200 mM NaCl) was measured at 40 °C, 800 MHz, using a pulse-acquire experiment. Experiments were performed for different tip angles (90°, 67.5°, 45°, 22.5° and 11.25°) and a variety of receiver gains (2, 1 and 0.5 on our system); with similar relative water concentrations obtained in all cases. The mean and standard deviations of these measurements are reported in the main text.

The CAPRIN1 concentration in the RNA:CAPRIN1 condensate of Figure 1 was measured at 40 °C, 800 MHz, using an excitation sculpting ^1H 1D experiment[12], by comparing the intensity of signals over a region extending from 0.9 ppm – 1.2 ppm to the intensity quantified in a reference CAPRIN1 condensed phase prepared (no RNA) with 400 mM NaCl, where the CAPRIN1 concentration was determined previously[13]. Similar experiments were performed using a simple pulse-acquire scheme and in both cases the relative CAPRIN1 concentrations determined were within experimental error.

NMR Data Analysis

(1) Thermodynamic and kinetic parameters

Fractional values of the population of ssRNA as a function of temperature (Figure 1D) were calculated from peak volumes in ddHMQC datasets using Eq. [S5] (below), with errors estimated by taking the standard deviation over multiple consecutive measurements. Effective ^{1}H relaxation rates ($R_{2,\text{eff}}$) used in Eq. [S5], were measured using the pulse scheme illustrated in Figure S5B, with peak intensities (obtained using *peakipy*) as a function of relaxation time fit to a mono-exponential decay function; errors in $R_{2,\text{eff}}$ were obtained via the covariance matrix approach[14]. The maximum single strand fraction in buffer (Figure 1D, grey) at an RNA concentration of 950 μM of each strand (same concentration as for condensate) was obtained by first estimating the ssRNA-dsRNA equilibrium constant at 65 °C from the ratio of ssRNA and dsRNA peak volumes (in a fully relaxed spectrum, using Eq. [S5]) along with the concentration of each ssRNA component in the buffer sample (100 μM) at 65 °C. Once the equilibrium constant was obtained (from a sample prepared with each strand at a total concentration of 100 μM) the concentration of each RNA component in a buffer comprised of total RNA strand concentrations of 950 μM was calculated.

Two magnetization exchange experiments (Figure 2, Figure S7), as described below, were recorded, from which the average of the standard deviation of volumes of corresponding peaks in each of the data sets was calculated to obtain the error, prior to averaging the data over both measurements. Errors in the volumes of peaks in the averaged dataset were obtained by dividing the peak errors in each of the two datasets by $\sqrt{2}$. Errors in the exchange parameters were estimated by using a Monte-Carlo approach[15], whereby 5,000 data sets were generated by sampling from a normal distribution with mean value equal to the experimental data points, and standard deviation equal to the error. The resulting peak volume vs. exchange time (T) profiles were fit to Eqs. [S2-S5] as described below, and the mean value and error in exchange parameters (computed as the standard deviation of the distribution) given in Tables S1 and S2 (condensate and buffer, 200 mM NaCl) and Figure S7 (buffer, 0 M NaCl). It should be noted that the ratio of the exchange rates ($k_{\text{ss-ds}}$ and $k_{\text{ds-ss}}$) was constrained to satisfy p_{ss} x $k_{\text{ss-ds}}$ = (1 – p_{ss}) x $k_{\text{ds-ss}}$, with p_{ss} obtained from Eq. [S5] (see below). Furthermore, cross-relaxation was not included when fitting the exchange data, as described below (see 'Measuring exchange parameters by analysis of diagonal peak intensities'). Simulations (Figure S8) establish that this omission does not impact the extracted exchange rates.

(2) Diffusion

Peak intensities (from either 1D or 2D spectra, see above), as a function of gradient strength, $I(G)$, were fit to $I(G) = I_0 e^{-DG^2(\kappa\gamma_H)^2\delta^2\Delta}$, where I_0 is the intensity at zero gradient strength, D is the diffusion coefficient (cm^2/s), G is the gradient strength in Gauss/cm, δ is the total duration of a pair of defocusing/refocusing bipolar gradients (s), Δ is the diffusion time (s), and κ is a scaling factor set to 1 (3) for the SQ (TQ) experiments. The

equation for $I(G)$ above is approximate[9], but for values of Δ on the order of hundreds of ms the error in D that results is negligible. Errors in D were obtained using the covariance matrix approach[14].

(3) Both strands of the duplex partition extensively into the condensed phase

In order to properly analyze and interpret the thermodynamic (Figure 1D) and kinetic (Figures 2B and 2C) data it is necessary to establish the extent to which both complementary RNA strands (Figure 1A) partition into the condensed phase of the phase separated sample. For example, a possible interpretation of the condensed phase profile of Figure 1D is that the 2'-O-methyl ($^{13}CH_3$) labeled strand partitions more extensively into the condensed phase than the unlabeled complementary strand, so that there will always be a baseline fraction of ssRNA (with methyl label) observed, in this case not reflective of the melting of the duplex. As only one of the two strands is 2'-O-methyl ($^{13}CH_3$) labeled, and, hence, NMR visible, we have prepared a second condensed phase sample, comprising complementary RNA strands where one is 2'-O-methyl labeled at the G position (G6), as before, and a second strand 2'-O-methyl labeled at the U position (U6), Figure S2A. We chose to modify a uridine on the complementary strand to minimize the extent of overlap between the methyl resonances. ddHMQC spectra of the double labeled RNA in buffer (100 μM in each RNA strand, 200 mM NaCl; at 57.5 °C, 800 MHz, Figure S2B, left; spectral acquisition time of 8 hr) show two resonances for the dsRNA arising from the G and U methyl groups, and a single resonance corresponding to the ssRNA arising from unresolved G and U methyls. These resonances are also observed in the condensed phase ddHMQC spectrum (Figure S2B, middle; spectral acquisition time of 8 hr). In contrast, resonances corresponding to either the dsRNA or ssRNA are not observed in the ddHMQC spectrum of the dilute phase (Figure S2B, right; spectral acquisition time of 16 h). Thus, both single strands partition extensively and similarly into the condensed phase.

(4) *Extracting RNA exchange parameters in the CAPRIN1 condensed phase*

(4.1) Limitations with traditional methods

Magnetization exchange experiments can, in principle, provide both the thermodynamic and kinetic parameters for systems undergoing conformational exchange. One powerful variant is based on recording [X-^{1}H] correlation maps where an exchange block of duration T is placed after the X chemical shift evolution period and before acquisition to produce a spectrum like that shown schematically in Figure S4A (left)[16-17]. By recording a series of 2D experiments as a function of T, a set of time dependent peak volume profiles is obtained that can be fit to extract the exchange kinetics of interest, Figure S4A (right).

Robust analysis of the data requires that differential relaxation of magnetization derived from each of the exchanging components be properly taken into account, but this is, in general, not limiting[18-19]. A complication occurs in cases where the X chemical shifts of the exchanging species are not sufficiently different so that cross-peaks become poorly resolved in the X dimension of 2D datasets, as illustrated in Figure S4B (left), for $T = 0$. In the example presented, the 'blue' ('green') peak derives from magnetization with short (relatively long) transverse relaxation times, as in the present application. Thus, for $T > 0$, it becomes difficult to reliably quantify cross-peak intensities (Figure S4B, right), since even slight artifacts from the intense diagonal peak ('green') would affect the weak ('blue' to 'green') cross-peak ('black'), and for short T values, especially, the cross-peak intensities would be significantly affected by the diagonal correlations. In some cases, a solution to the problem would be to record [^{1}H-^{1}H] versions of the experiment, so long as resolution in the ^{1}H dimension is adequate, as we[20] and others[17] have done previously in studies of different systems. In the application considered here, however, the 2'-O-methyl ^{1}H peak is obscured by the CAPRIN1 proton spectrum and it would not be possible to quantify correlations in such homonuclear spectra.

[^{13}C-^{1}H] magnetization exchange spectra recorded on the RNA:CAPRIN1 condensate (57.5 °C, 800 MHz) are illustrated in Figure S4C, $T = 0.9$ ms (left) and $T = 15$ ms (right), highlighting the challenges described above. In particular, the ssRNA is dynamic with effective transverse relaxation rates during both t_1 and t_2 that are relatively small (^{1}H $R_{2,\text{eff}} = 28.9 \pm 0.7$ s^{-1}, 57.5 °C, 800 MHz). Notably, a trace at the ^{1}H frequency of the ssRNA 2'-O-methyl proton in a [^{13}C, ^{1}H] F_1-coupled HSQC spectrum has a multiplet structure of 3.2:1:1:2.6 (downfield to upfield in ^{13}C), which is close to the 3:1:1:3 multiplet volume ratio that would be expected in the case of a molecule with rapid tumbling (Figure S4D, right), and in the absence of cross-correlated relaxation between ^{1}H-^{13}C dipole - ^{13}C CSA relaxation interactions[21]. The corresponding trace through the dsRNA peak has a multiplet structure of approximately 4.5:4.5:2.4:1 (downfield to upfield in ^{13}C; Figure S4D, left), indicating that the dsRNA tumbles more slowly, as might be expected for a rigid structure with more efficient relaxation (^{1}H $R_{2,\text{eff}} = 133.6 \pm 0.6$ s^{-1}, 57.5 °C, 800 MHz). The significant imbalance in R_2 values complicates recording spectra that are simultaneously optimal for both peaks. Long acquisition times in t_1 would be appropriate for the ssRNA correlation and, importantly, minimize sinc wiggles in the ^{13}C frequency domain that complicate extraction of cross-peak intensities reporting on magnetization exchange from dsRNA to ssRNA. However, this would lead to a reduction in the signal-to-noise of the dsRNA peak that is of low sensitivity in the first place. An additional complication arises from the fact that the longitudinal relaxation rate for the dsRNA component is approximately an order of magnitude faster than the exchange kinetics so that the buildup of cross-peak intensities becomes severely attenuated (Table S1). Attempts to record accurate exchange kinetics using the 'traditional' [X-^{1}H] pseudo-3D approach have, therefore, failed.

(4.2) *Measuring exchange parameters by analysis of diagonal peak intensities*

Figure S5A shows the ddHSQC based pulse sequence that has been developed to quantify exchange in the RNA:CAPRIN1 condensed phase of interest here. Exchange parameters are extracted from simultaneous fits of data recorded with the exchange block (*T*) placed either before or after recording ^{13}C chemical shift (t_1), focusing on the diagonal peaks. The evolution of magnetization during each of the experiments can be described succinctly by,

$$I_z \rightarrow 2I_zC_z \rightarrow T \rightarrow t_1(^{13}\text{C}) \rightarrow dd\text{-}t_2(^{1}\text{H}) \qquad \text{[S1a]}$$

and

$$I_z \rightarrow 2I_zC_z \rightarrow t_1(^{13}\text{C}) \rightarrow T \rightarrow dd\text{-}t_2(^{1}\text{H}) \qquad \text{[S1b]}$$

for the 'before' ([S1a]) and 'after' ([S1b]) experiments, where X_j is the j^{th} component $j \in (x,y,z)$ of X angular momentum, $2I_zC_z$ is longitudinal order that exchanges between states during T, t_j is an evolution time for the spin of interest (indicated in parenthesis), and '*dd*' indicates that the delayed decoupling approach is used. The RNA studied here (Figure 1A) is fully protonated so that cross relaxation between protons is operative (and efficient in the case of dsRNA, see below). Careful design of the exchange experiments is, thus, required, to minimize the effects of cross relaxation and the multi-exponential decay behaviour that would ensue. This can be achieved by ensuring that only magnetization derived from the 2'-O-methyl group is present at the start of *T*, as then cross relaxation that couples the evolution of proximal *I* and *S* proton spins is suppressed for initial *T* values[22]. As the RNA is not ^{13}C labeled, with the exception of the methyl group, such a scenario is realized by generating $2I_zC_z$ as the initial magnetization state. The effects of different boundary conditions on relaxation measurements have been discussed in detail previously[22-23].

Figure S6A shows schematics of a pair of 'before' and 'after' [^{13}C-^{1}H] magnetization exchange planes recorded for $T > 0$, where cross-peaks are observed only in the 'after' case. Magnetization exchange does occur during *T* in the 'before' experiment as well, however, each of the peaks in this spectrum can be thought of as a 'composite peak', with the volume of the dsRNA correlation (V'_{ds}), for example, given by the sum of contributions from magnetization 'residing' on dsRNA during *T* or transferred from ssRNA to dsRNA during *T*, $V'_{ds} = V_{ds,ds} + V_{ss,ds}$ where V'_i and $V_{i,j}$ are defined as in the figure, with $V_{i,j}$ the volume of a cross-peak, $i \neq j$, (diagonal peak, $i=j$) in the 'after' experiment derived from magnetization flowing from state *i* to *j* during *T* (or in the case of the diagonal peak magnetization associated with state *i* throughout). In the approach below, only the diagonal peaks are used in the analysis. Because for the *T* values chosen the diagonal

peaks are, in general, more intense than the cross-peaks, especially for the intense single strand diagonal in the condensed phase that obscures the dsRNA→ssRNA cross-peak (Figure S4C), the diagonal peaks can be quantified much more accurately than the corresponding correlations associated with the (small) cross-peaks arising from magnetization transfer.

It can be shown that in the limit of short *T*, assuming fully relaxed spectra, and neglecting differential transverse relaxation during the course of the experiment, the Volume *vs T* profiles in the 'before' and 'after' experiments are single exponential, for example, $V'_{ds}(t) = V'_{ds}(0)e^{-R_{1zz,ds}T}$ and $V_{ds,ds}(t) = V_{ds,ds}(0)e^{-((R_{1zz,ds}+k_{ds-ss})T)}$ for the dsRNA peaks in the 'before' and 'after' cases, respectively, where $R_{1zz,ds}$ is the relaxation rate for longitudinal order, $2I_zC_z$, for the dsRNA resonance, and $k_{ds\text{-}ss}$, is the exchange rate from dsRNA to ssRNA. The expression for $V'_{ds}(t)$ does not depend on the rates of exchange, as magnetization that is transferred from dsRNA to ssRNA is fully compensated by reverse transfer from ssRNA to dsRNA, for short delay times. Interestingly, in the limit where $R_{1zz,ds} = R_{1zz,ss}$, and starting from equilibrium magnetization, $V'_{ds}(t)$ evolves independently of the exchange rates for all *T*. Decay profiles for diagonal peaks are illustrated in Figure S6B for both ssRNA and dsRNA, calculated using relaxation and exchange parameters similar to those measured in the condensed phase sample (Table S1). Notably, the decays for the correlations in the 'before' experiments are slower than the corresponding decays in the 'after' datasets, as expected, since magnetization that flows from state A to state B in this case is replenished from the reverse flow (but not for the 'after' experiment).

Assuming that the 2'-O-methyl group is isolated (no cross relaxation), that fully relaxed spectra have been recorded, and finally, neglecting the effects of differential transverse relaxation for dsRNA and ssRNA resonances during the course of the experiments, the general equations that describe two-site magnetization exchange during *T* are biexponential and given by the following expressions that follow directly from Farrow *et al* [16]:

$$V_{ds,ds}(t) = V_{ds}(0)M_{ds,ds}(t)$$

$$V_{ss,ss}(t) = V_{ss}(0)M_{ss,ss}(t)$$

$$V_{ss,ds}(t) = V_{ss}(0)M_{ss,ds}(t)$$

$$V_{ds,ss}(t) = V_{ds}(0)M_{ds,ss}(t)$$

where,

$$M_{ds,ds}(t) = \frac{(-(\lambda_2 - a_{11})e^{-\lambda_1 t}) + ((\lambda_1 - a_{11})e^{-\lambda_2 t})}{\lambda_1 - \lambda_2}$$

$$M_{ss,ss}(t) = \frac{(-(\lambda_2 - a_{22})e^{-\lambda_1 t}) + ((\lambda_1 - a_{22})e^{-\lambda_2 t})}{\lambda_1 - \lambda_2}$$

$$M_{ss,ds}(t) = \frac{(-a_{12}e^{-\lambda_2 t} + a_{12}e^{-\lambda_1 t})}{\lambda_1 - \lambda_2}$$

$$M_{ds,ss}(t) = \frac{(-a_{21}e^{-\lambda_2 t} + a_{21}e^{-\lambda_1 t})}{\lambda_1 - \lambda_2}$$

and

$$V'_{ds}(t) = V_{ds,ds}(t) + V_{ss,ds}(t)$$

$$V'_{ss}(t) = V_{ss,ss}(t) + V_{ds,ss}(t) \qquad \text{[S2]}$$

In Eq. [S2],

$$a_{11} = R_{1zz,ds} + k_{ds-ss},\ a_{12} = -k_{ss-ds},\ a_{21} = -k_{ds-ss},\ a_{22} = R_{1zz,ss} + k_{ss-ds}$$

$$\lambda_1 = \frac{1}{2}(a_{11} + a_{22} + \sqrt{(a_{11} - a_{22})^2 + (4k_{ss-ds}k_{ds-ss})})$$

$$\lambda_2 = \frac{1}{2}(a_{11} + a_{22} - \sqrt{(a_{11} - a_{22})^2 + (4k_{ss-ds}k_{ds-ss})}) \qquad \text{[S3]}$$

V_i(t) are the 'equilibrium' volumes of the diagonal/cross peaks (Figure S6A), $k_{i\text{-}j}$ is the rate of exchange from state *i* to state *j*, and $V_{ds}(0)$ and $V_{ss}(0)$ quantify the 'amount' of longitudinal order for the dsRNA and ssRNA species at the start of the magnetization exchange period, $k_{ss\text{-}ds} = k_{on}[ss]$, where k_{on} is the bimolecular association rate constant (in $M^{-1}s^{-1}$), and [ss] is the concentration of the unlabeled strand complementary to the methylated strand, $k_{ds\text{-}ss} = k_{off}$ (Figure 2A). The two single strands are shown to partition similarly into the condensed phase, as described in Figure S2. Thus, [ss] can be reliably obtained from measurements of the population of the methylated single strand (p_{ss}, see below), as $p_{ss}*C_t$, where C_t is the total concentration of labeled RNA in the condensate/buffer. In this way k_{on} and k_{off} are extracted from the magnetization exchange experiments described above, along with relaxation rates of longitudinal order $2I_zC_z$ ($R_{1zz,ds}$, $R_{1zz,ss}$) and initial volumes ($V_{ds}(0)$, $V_{ss}(0)$) that are also treated as fitting parameters. Usually, exchange parameters from magnetization exchange experiments are obtained by fitting the variation of cross- and diagonal peak volumes in the 'after' experiment as a function of time, however, for reasons described above the time variation of the diagonal peaks, $V'_{ds}(t)$ and $V'_{ss}(t)$ in the 'before', and $V_{ds,ds}(t)$ and $V_{ss,ss}(t)$ in the 'after' experiments are analyzed in our study.

The assumptions for which Eq. [S2] hold are not valid for the exchanging RNA system considered here as ^1H and ^{13}C transverse and longitudinal relaxation rates differ

for the ssRNA and dsRNA species. Thus, the magnetization of both RNA species at the start of the exchange block are affected by relaxation which must, therefore, be explicitly taken into account. Assuming for the moment that the 2'-O-methyl group is isolated (no cross relaxation), the time dependencies of the 'before' ($V'_{ds}(t)$,$V'_{ss}(t)$) and 'after' ($V_{ds,ds}(t), V_{ss,ss}(t)$) (see Figure 6A) diagonal peaks are given by:

$$V_{ds,ds}(t) = \kappa_{ds} V_{ds}(0) M_{ds,ds}(t)$$

$$V_{ss,ss}(t) = \kappa_{ss} V_{ss}(0) M_{ss,ss}(t)$$

$$V'_{ds}(t) = \kappa_{ds}(V_{ds}(0) M_{ds,ds}(t) + V_{ss}(0) M_{ss,ds}(t))$$

$$V'_{ss}(t) = \kappa_{ss}(V_{ss}(0) M_{ss,ss}(t) + V_{ds}(0) M_{ds,ss}(t)) \qquad \text{[S4a]}$$

where,

$$V_{ds}(0) = p_{ds} e^{-R_{2eff,ds} * 2\tau_a} \left(\frac{V_{ds,D1=D1ex}}{V_{ds,D1=15s}}\right)$$

$$V_{ss}(0) = p_{ss} e^{-R_{2eff,ss} * 2\tau_a} \left(\frac{V_{ss,D1=D1ex}}{V_{ss,D1=15s}}\right) \qquad \text{[S4b]}$$

In Eq. [S4a] κ_i ($i \in$ {ss,ds}) is a fitting parameter proportional to the total equilibrium magnetization in the sample (sum over ssRNA and dsRNA) and, includes the effects of transverse relaxation of state *i* during all delays in the pulse scheme with the exception of the first INEPT period ($2\tau_a$; explicitly taken into account via the exponential term in Eq. [S4b], see Figure S5A); $p_{ds} = 1 - p_{ss}$ ($R_{2eff,ds}$) and p_{ss} ($R_{2eff,ss}$) are the populations (effective ^{1}H transverse relaxation rates) of the dsRNA and ssRNA species, respectively; $V_{i,D1}$ is the volume of the methyl peak corresponding to species $i \in$ {ss,ds}, as measured in a ddHMQC experiment recorded with a recycle delay of D1; $D1_{ex}$ is the recycle delay used in the magnetization exchange experiments (typically 1.5-3 s). The exponential ($e^{-R_{2eff,i} * 2\tau_a}$) and ($\frac{V_{i,D1=D1ex}}{V_{i,D1=15s}}$) terms in Eq. [S4b] account for differences in transverse and longitudinal ^{1}H relaxation rates, respectively, between ssRNA and dsRNA, with the latter term correcting for the fact that spectra recorded for the magnetization exchange experiment are not fully relaxed. It is important to note that in the derivation of Eq. [S4] we have assumed that chemical exchange occurs during *T* and not during the small, fixed delays in the rest of the experiment during which gradients are applied or magnetization evolves due to scalar couplings, for example. Finally, peak intensities can be used in the analysis instead of volumes, as this will only affect the κ_i factors in Eq. [S4].

Effective ^{1}H R_2 values that are input into Eq. [S4b] were measured for ssRNA and dsRNA using the pulse scheme of Figure S5B. In turn, p_{ds} and p_{ss} were quantified by measuring peak volumes (V_i) in fully relaxed ddHMQC experiments (typically with recycle

delays of 15s), and accounting for differences in transverse relaxation rates between both species during delays in the experiment, as follows:

$$p_i = \frac{\frac{V_i}{e^{-R_{2eff,i}*t_{seq}}}}{\sum_i^q \frac{V_i}{e^{-R_{2eff,i}*t_{seq}}}} \qquad [S5]$$

where t_{seq} is the length of all delays during the ddHMQC experiment, equal to $\tau_a + \tau_b + 2T' + 2G_3$, as defined Figure S5B, and the summation in the denominator is over the dsRNA and ssRNA species, taking into account the appropriate transverse relaxation rates. The obtained populations are used to constrain the exchange rates (Eq. [S3]) in fits of the data (Figure 2, Figure S7, Tables S1 and S2, see below) via the relation $(1 - p_{ss}) \times k_{ds\text{-}ss} = p_{ss} \times k_{ss\text{-}ds}$. In Eq. [S5] we have assumed that the relaxation of ^{1}H single and ^{1}H-^{13}C multiple quantum coherences for a given RNA species are the same; this simplification is unlikely to introduce significant error as the fixed time delays in the experiment are small (for example, ~0.9 ms fixed delay during which multiple quantum coherences evolve during application of coherence transfer selection gradients).

The denominator of Eq. [S5] when summed over the dsRNA and ssRNA peaks in the condensed phase, gives the net amount of labeled RNA, and can be compared to the corresponding total peak volume obtained using a buffer sample of fixed RNA concentration (100 μM in our case) to then obtain the total concentration of labeled RNA (C_t) in the condensed phase, and consequently [ss] and k_{on} (see above). C_t for the buffer sample (100 μM) can be measured using the extinction coefficient of the RNA as described in Materials and Methods.

We have validated this methodology by recording ‘before’ and ‘after’ experiments on a 100 μM RNA sample (each strand of the duplex in Figure 1A at 100 μM; 0 mM NaCl), at 57.5 °C, 800 MHz. Exchange parameters obtained by simultaneous fits of the diagonal peaks in ‘before’ and ‘after’ experiments to Eqs. [S2-S5] were compared with simultaneous fits of cross and diagonal peaks in the ‘after’ dataset (Eqs. [S2-S3]), and are in excellent agreement with each other (Figure S7).

The above discussion has neglected the effects of cross relaxation between the 2'-O-methyl group protons and non-methyl proximal proton spins. Although the boundary conditions for magnetization at $T = 0$ are such that cross relaxation effects are minimal for initial T values, and we have chosen relatively short exchange delays, T (≤ 60ms in the condensed phase), cross relaxation could, nevertheless, influence the extracted exchange parameters, in particular, when using data from the dsRNA that tumbles more slowly than the ssRNA in the condensed phase (Figure S4D). In particular, the H1' and H2' sugar protons are at average distances of 3 Å and 2.8 Å from the methyl protons, so that efficient cross relaxation pathways are present, and these may well be significant for larger T values and for the slowly tumbling dsRNA in the condensed phase.

In order to establish whether robust measures of exchange rates can be obtained by neglecting cross relaxation in fits of the experimental data, a series of simulations have been performed, guided by experiment. The rationale is to generate simulated data that includes cross relaxation, fit the data assuming no cross relaxation, as is done for the experimental data in this study, and check the similarity of the fitted/extracted parameters to the input values.

As a first step, the experimental condensed phase 'before' and 'after' data (extending to T = 60 ms) were fit using a model that does not include cross relaxation (this is the case in all fits considered in this work) using Eqs. [S2-S5] (Figure 2) to extract exchange rates and $V(0)$ values which were subsequently used in the analysis (k_{ds-ss}^{expt}= 2.9 s^{-1}; k_{ss-ds}^{expt}= 0.6 s^{-1}, $R_{1zz,ds}^{expt}$= 17.2 s^{-1}, $R_{1zz,ss}^{expt}$= 3.1 s^{-1}, Table S1). Figure S8A (left two columns) shows simulated data (no cross relaxation) generated with parameters obtained from such fits as a baseline for subsequent computations (data from 'before' and 'after' diagonal peaks are colored black and blue, respectively). Simulated profiles for both dsRNA and ssRNA (indicated by 'ss&ds') for T values extending to either 60 ms or 15 ms were subsequently analyzed to obtain fit parameters (using Eqs. [S2-S5], blue and orange bars in Figure S8A, 3rd to 6th columns). Also shown in green are exponential fits to the ds (ds-after, T=15ms) or ss (ss-after, T=15ms) diagonal peaks in the 'after' experiment for T extending to 15ms, to extract $k_{ds\text{-}ss}$ + $R_{1zz,ds}$ (dsRNA) or $k_{ss\text{-}ds}$ + $R_{1zz,ss}$ (ssRNA) (see initial time limit expressions above and Figure S6B; Figure S8A, 3rd and 4th columns). As expected, given that the simulations are performed in the absence of error, excellent agreement between the input (dashed horizontal lines) and output fit parameters (bars) was obtained.

Next, we simulated data that included cross relaxation (see Eq. [S6] below; Figure S8B, left two columns). As an initial 'guess' for parameters, including cross relaxation rates and relaxation rates of longitudinal order (R_{1zz}) for these simulations, that approximate the values operative for the experimental data, we measured the decay of dsRNA and ssRNA diagonal peaks in the 'after' experiment recorded using T values up to 15 ms (see below). For short delays, such that $|\sigma T| < 1$, the decay of a diagonal correlation in the 'after' experiment is reasonably well approximated by a single exponential, with an extracted rate for the dsRNA and ssRNA diagonal peaks of ~($k_{ds-ss}^{expt,single-exp}$+$R_{1zz,ds}^{expt,single-exp}$) and ~($k_{ss-ds}^{expt,single-exp}$+$R_{1zz,ss}^{expt,single-exp}$), respectively, when fit in this manner. The superscripts '*expt,single-exp*' (above) indicate that experimental data is fit to a single exponential decay, as opposed to fits using Eqs. [S2-S5] of simulated profiles in which case superscript '*expt*' is replaced by superscript '*sim*' below (to indicate fits of the complete simulated dataset). From the extracted $k^{expt,single-exp}$ + $R_{1zz}^{expt,single-exp}$ values and the fitted k_{ds-ss}^{expt} and k_{ss-ds}^{expt} rates (Table S1) appropriate values for $R_{1zz,ds}$ (26 s^{-1}) and $R_{1zz,ss}$ (3.0 s^{-1}) are obtained. These values are

then used in simulations of the evolution of the longitudinal order terms for dsRNA and ssRNA, $2I_zC_{z,ds}$ and $2I_zC_{z,ss}$, respectively, as a function of *T*, for different values of cross relaxation rates, σ_{ds} and σ_{ss}, that couple spins *I* and *S* (external spin) using Eq. [S6]:

$$\frac{d}{dt}\begin{bmatrix}2I_zC_{z,ds}\\2S_zC_{z,ds}\\2I_zC_{z,ss}\\2S_zC_{z,ss}\end{bmatrix}=\begin{bmatrix}-k_{ds-ss}-R_{1zz,ds} & -3\sigma_{ds} & k_{ss-ds} & 0\\ -\sigma_{ds} & -k_{ds-ss}-R_{1,SzCz,ds} & 0 & k_{ss-ds}\\ k_{ds-ss} & 0 & -k_{ss-ds}-R_{1zz,ss} & -3\sigma_{ss}\\ 0 & k_{ds-ss} & -\sigma_{ss} & -k_{ss-ds}-R_{1,SzCz,ss}\end{bmatrix}\begin{bmatrix}2I_zC_{z,ds}\\2S_zC_{z,ds}\\2I_zC_{z,ss}\\2S_zC_{z,ss}\end{bmatrix} \quad \text{[S6]}$$

In Eq. [S6] we have assumed that the methyl protons (spin *I*, where *I* is the sum over the three equivalent protons) are proximal to a single external proton *S* and the factor of three in some of the cross relaxation terms takes into account that there are three methyl protons and only a single *S* proton. Note that $R_{1,SzCz,ds} = R_{1,SzCz,ds}^{intrinsic} - 3\sigma_{ds}$ and $R_{1,SzCz,ss} = R_{1,SzCz,ss}^{intrinsic} - 3\sigma_{ss}$, where $R_j^{intrinsic}$ is the relaxation rate including all contributions with the exception of those from the proximal methyl protons and $\sigma < 0$ (the factor of 3 accounts for the 3 methyl protons that relax spin S). Thus, the minimum values for $R_{1,SzCz,ds}$ and $R_{1,SzCz,ss}$ are $-3\sigma_{ds}$ and $-3\sigma_{ss}$, respectively. The value of σ_{ss} was constrained such that ($\sigma_{ss}=\sigma_{ds}*R_{1,SzCz,ss}/R_{1,SzCz,ds}$). The simulated data (using Eq. [S6]) were subsequently fit to expressions that neglect cross relaxation (Eqs. [S2-S5]) and values of σ_{ds}, σ_{ss}, $R_{1,SzCz,ds}$, and $R_{1,SzCz,ss}$ modified in a series of iterations, ensuring that $R_{1,SzCz,ds}$ ($R_{1,SzCz,ss}$) ≥ $-3\sigma_{ds}$ ($-3\sigma_{ss}$) (see above), until the extracted rates ($k_{ds-ss}^{sim} + R_{1zz,ds}^{sim}$) and ($k_{ss-ds}^{sim} + R_{1zz,ss}^{sim}$) agreed with those obtained from fits of the experimental data extending to *T* = 60 ms ($k_{ds-ss}^{expt} + R_{1zz,ds}^{expt}$ and $k_{ss-ds}^{expt} + R_{1zz,ss}^{expt}$, Table S1). The parameters so generated (σ_{ds}=-13.8 s^{-1} and σ_{ss}=-1.1 s^{-1}, $R_{1,SzCz,ds}$ = 50 s^{-1} and $R_{1,SzCz,ss}$=4 s^{-1}) were then used to simulate decay profiles for diagonal peaks (Figure S8B, left two columns) which were subsequently fit to expressions that neglect cross relaxation (Eqs. [S2-S5], Figure S8B, 3rd to 6th columns). Recall that we have 'adjusted' σ_{ds} values in our simulations so that the fitted values ($k_{ds-ss}^{sim} + R_{1zz,ds}^{sim}$) and ($k_{ss-ds}^{sim} + R_{1zz,ss}^{sim}$) agree well with those obtained experimentally (*T* = 60 ms), as can be observed by comparing the blue bar and dashed horizontal line (which corresponds to the fitted parameters from experiment; Figure S8B, 3rd and 4th columns). Note, however, that for *T* = 15 ms the fitted ($k_{ds-ss}^{sim} + R_{1zz,ds}^{sim}$) rate is larger (orange bar, Figure S8B, 3rd column), and so is the rate obtained from an exponential fit to the dsRNA diagonal intensity profile in the 'after' experiment (green bar, Figure S8B, 3rd column). In multi-exponential systems, such as in a system with cross relaxation, the fitted decay rates when cross relaxation is neglected decrease with increasing *T* since the influence of the slower relaxing components become more pronounced with time. In contrast, less of an effect is observed for the ($k_{ss-ds}^{sim} + R_{1zz,ss}^{sim}$) rate (Figure S8B, 4th column) because $|\sigma_{ss}| \ll |\sigma_{ds}|$, reflecting the increased level of dynamics of ssRNA relative to dsRNA (Figure S4D). Notably, the fitted k_{ds-ss}^{sim} and k_{ss-ds}^{sim} values are in excellent agreement with the input kinetic rates, establishing that, at least in the RNA:CAPRIN1 condensed phase system considered here, robust kinetic parameters

can be obtained by fitting relaxation data that includes cross relaxation to a model where cross relaxation is neglected (Figure S8B, 5th and 6th columns). Figure S8C shows distributions of extracted parameters based on fits of simulated data with cross relaxation (using ss and ds diagonals for *T*=60ms), including errors comparable to those obtained experimentally, and with the dashed vertical lines denoting the values obtained from analysis of experimental data (Table S1). The distribution of kinetic rates so obtained suggests that the errors in experimental data could influence the extracted kinetic rates by ~2-fold, but such changes do not affect the conclusions of our study. Finally, Figure S8D compares exchange parameters obtained from a fit of experimental data (k_{ds-ss}^{expt} + $R_{1zz,ds}^{expt}$) and (k_{ss-ds}^{expt} + $R_{1zz,ss}^{expt}$) out to *T*=60ms (blue), versus those obtained from single exponential fits to the experimental 'after' data extending to *T* = 15ms (columns 1 and 2) to extract values of $k_{ds-ss}^{expt,single-exp}$+$R_{1zz,ds}^{expt,single-exp}$ and $k_{ss-ds}^{expt,single-exp}$+$R_{1zz,ss}^{expt,single-exp}$ (green in columns 3 and 4). As expected, for ssRNA, both quantities are in agreement with each other (compare blue and green in columns 3 and 4), as there is less cross relaxation, while for dsRNA, the values obtained from *T*=15ms are larger. Thus, increasing extracted relaxation rates as *T* decreases is the hallmark of cross relaxation.

We have also repeated the analysis described above using additional (k_{ds-ss}, k_{ss-ds}) values, including (4.0 s^{-1}, 0.9 s^{-1}), and (1.6 s^{-1}, 0.3 s^{-1}), which were obtained by fitting experimental data corresponding to only the dsRNA or ssRNA diagonal peaks, while ensuring that the measured equilibrium ratio of ssRNA and dsRNA is maintained. Notably, values of exchange rates obtained in all cases agree well with input values.

To further quantify the errors associated with neglecting cross relaxation in our analyses above we have performed additional simulations for various values of kinetic parameters and cross relaxation rates. Starting from the parameters used to generate the profiles in Figure S8B ($R_{1,SzCz,ds}$=50 s^{-1}, $R_{1,SzCz,ss}$=4s^{-1}, $R_{1zz,ds}$=26 s^{-1}, $R_{1zz,ss}$=3.0 s^{-1}, σ_{ds}=-13.8 s^{-1} and σ_{ss}=-1.1 s^{-1}), values of $R_{1,SzCz,ds}^{intrinsic}$=$R_{1,SzCz,ds}$+3$\sigma_{ds}$=8.6 s^{-1}, $R_{1,SzCz,ss}^{intrinsic}$=$R_{1,SzCz,ss}$+3$\sigma_{ss}$=0.7 s^{-1}, $R_{1,IzCz,ds}^{intrinsic}$=$R_{1zz,ds}$+$\sigma_{ds}$=12.2 s^{-1} and $R_{1,IzCz,ss}^{intrinsic}$=$R_{1zz,ss}$+$\sigma_{ss}$=2.0 s^{-1} were calculated. The value of σ_{ds} was subsequently varied from 0 s^{-1} to 20 s^{-1}, in steps of 0.5 s^{-1}, keeping the intrinsic relaxation rates fixed to the values above (i.e., only methyl-S relaxation contributions were allowed to vary- all other contributions are fixed), while constraining $\sigma_{ss} = \sigma_{ds} * R_{1,SzCz,ss}^{intrinsic} / R_{1,SzCz,ds}^{intrinsic}$. For each value of σ_{ds}, k_{ds-ss} was varied from 1.0 s^{-1} to 11 s^{-1} in steps of 0.5 s^{-1}, while constraining k_{ss-ds} using the relation p_{ss} x k_{ss-ds} = (1 – p_{ss}) x k_{ds-ss}, as described above. Profiles extending to *T*=60ms were calculated (using Eq. [S6]) for the duplex and single strand diagonal peaks for the 'before' and 'after' experiments and subsequently fit to Eqs. [S2-S5] which neglect cross relaxation. The resulting exchange parameters were within 10% of the ground truth values used as input to the simulations. Similar observations were also made by either increasing or decreasing the intrinsic relaxation rates for the external

proton by 3-fold. Finally, our simulations establish that more robust values of exchange rates are extracted when 'before' and 'after' peaks for dsRNA and ssRNA are fit simultaneously, as has been done here.

(4.3) *Extraction of exchange parameters in buffer*

Figure 2B shows decay profiles from 'before' and 'after' experiments recorded for the dsRNA peak in a buffer solution, 200 mM NaCl, 57.5 °C. Under these conditions the dsRNA/ssRNA equilibrium heavily favors the duplex conformer, the ssRNA peak is, therefore, very weak (inset) and it is not possible to accurately quantify it during the course of the magnetization exchange experiment. In contrast, the dsRNA correlations are very strong and can be quantified with low errors. Simulations establish that accurate values of kinetic parameters can be extracted with this limited data so long as the relaxation rate of ssRNA longitudinal order can be measured, as well as the ratio of dsRNA and ssRNA concentrations in the sample. We have carried out the former measurement using a sample where only the $^{13}CH_3$ labeled single strand is present (i.e., no complementary strand; 25 μM RNA in 10 mM sodium phosphate, 10% D_2O, pH 7.0, 200 mM NaCl). The ratio of dsRNA to ssRNA can be obtained from a fully relaxed and highly sensitive ddHMQC experiment recorded on the sample used to measure exchange. These parameters were subsequently used in fits of the data to Eqs. [S2-S5] (Table S2).

Parameter	Fit Value
k_{on}^{expt} ($M^{-1}s^{-1}$)	810 ± 120
k_{off}^{expt} (s^{-1})	2.9 ± 0.4
$R_{1zz,ds}^{expt}$ (s^{-1})	17.2 ± 0.9
R_{1zz}^{expt} (s^{-1})	3.1 ± 0.1

Table S1. Exchange parameters obtained from fitting the magnetization exchange data for the RNA (Figure 1A) in condensed phase at 57.5 °C and 800 MHz (0.95 mM of both RNA strands in 10 mM sodium phosphate, 200 mM NaCl, 10% D_2O, pH 7.0) (Figure 2B, 'Condensed'). Errors for the fitted parameters were obtained using a Monte-Carlo procedure as described in Materials and Methods.

Parameter	Fit Value
k_{on}^{expt} ($M^{-1}s^{-1}$)	$2.2 \pm 0.5 \times 10^5$
k_{off}^{expt} (s^{-1})	0.2 ± 0.1
$R_{1zz,ds}^{expt}$ (s^{-1})	2.2 ± 0.1
R_{1zz}^{expt} (s^{-1})*	1.9

Table S2. Exchange parameters obtained from fitting the magnetization exchange data for the RNA (Figure 1A) in buffer at 57.5 °C and 800 MHz (100 μM dsRNA in 10 mM sodium phosphate, 200 mM NaCl, 10% D_2O, pH 7.0) (Figure 2B, 'Buffer'). Errors for the fitted parameters were obtained using a Monte-Carlo procedure as described in Materials and Methods. * denotes value fixed during the fit, obtained from a magnetization exchange experiment on a single strand RNA sample (25 μM RNA in 10 mM sodium phosphate, 200 mM NaCl, 10% D_2O, pH 7.0 at 57.5 °C and 800MHz). See '*Extraction of exchange parameters in buffer*'.

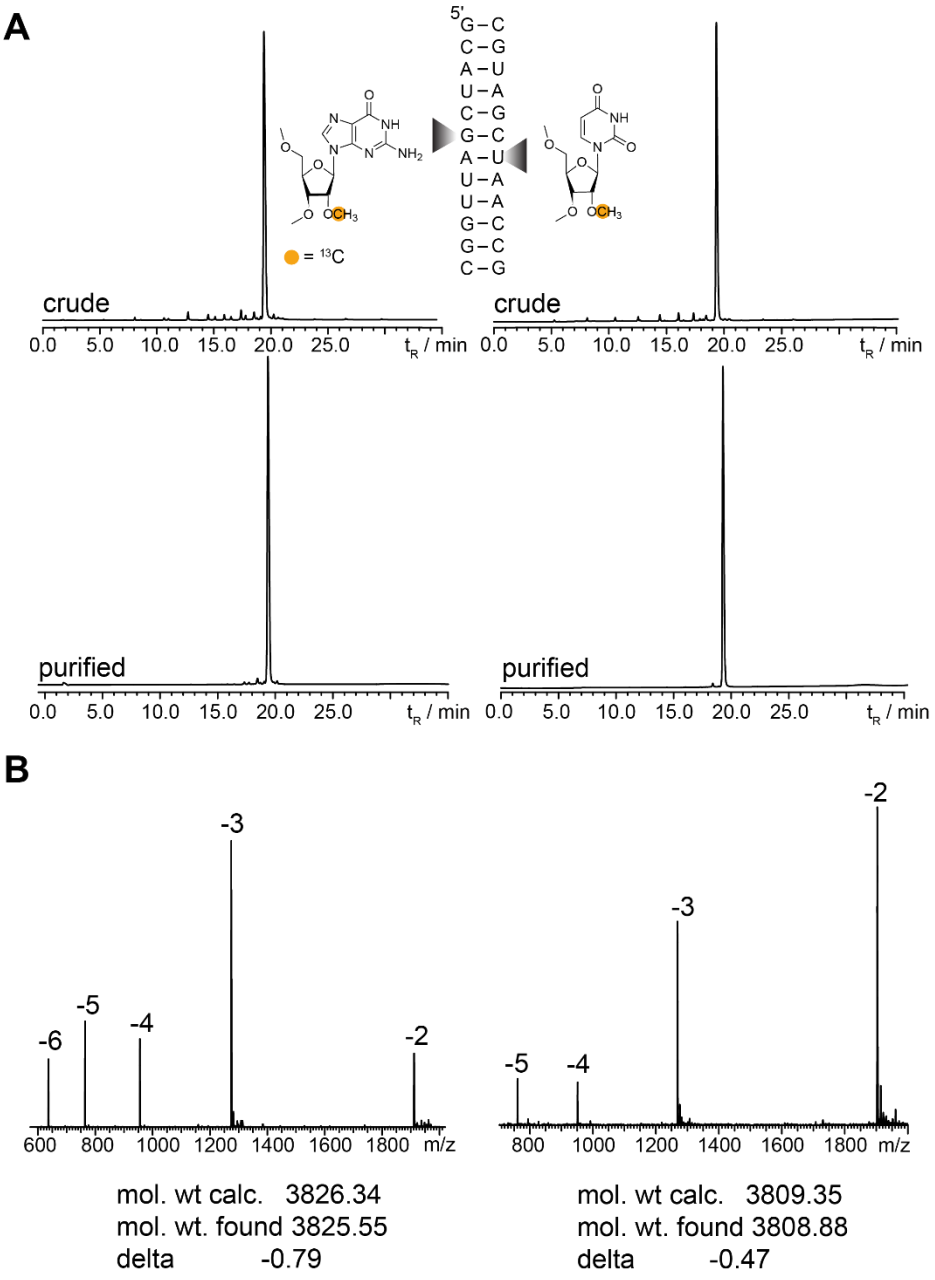

Figure S1. High quality synthesis of 2'-O-methyl labeled RNAs. (A) Anion exchange chromatograms of crude and purified 2'-O-methyl labeled RNAs, where t_R refers to retention time. (B) LC-ESI MS data of synthesized RNAs.

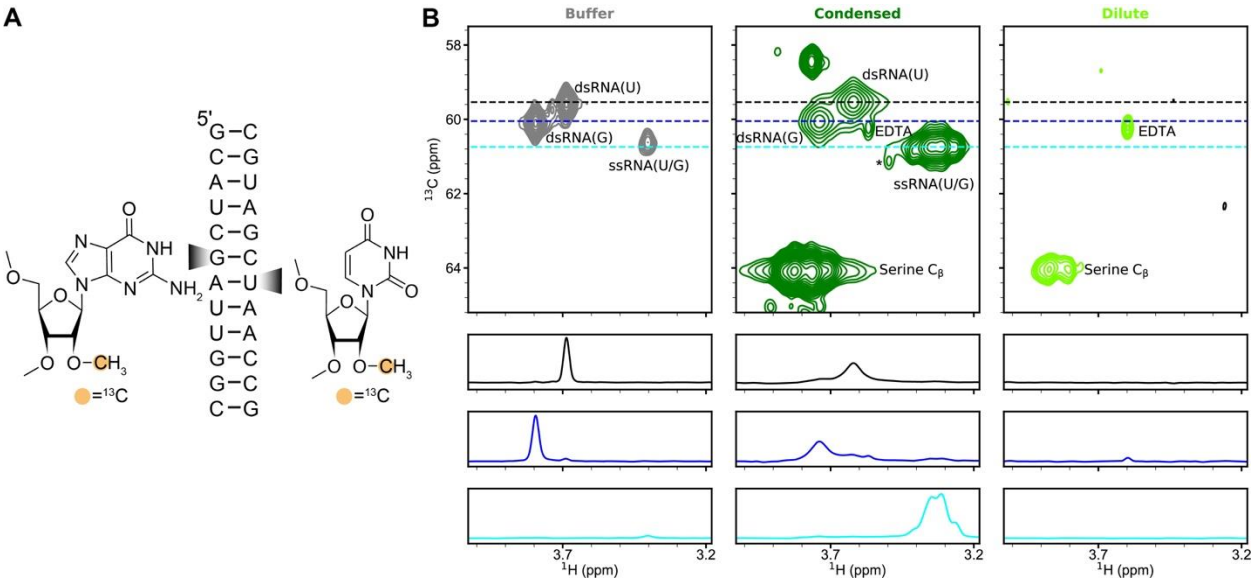

Figure S2. (A) Secondary structure of the RNA duplex with 2'-O-methyl modifications at the indicated guanosine and uridine residue on both strands of the duplex. The methyl groups are ^{13}C labeled. (B) Fully relaxed ddHMQC spectra (d1=15s, collected with identical acquisition parameters) of the RNA in buffer (gray, left), condensed phase (green, middle) and dilute phase (light green, right). The positions of the methyl resonances arising from the RNA are highlighted, as well as those from the C_β groups of serine residues of natural abundance CAPRIN1. There are no observable 2'-O-methyl resonances in the dilute phase within detection limits, suggesting that both single strands partition extensively and comparably into the condensed phase. There is a minor peak arising from EDTA in the 'Condensed' and 'Dilute' panels, a trace amount of which was remaining in the buffer after exchanging CAPRIN1. The minor peak (*) in the 'Condensed' panel arises from the guanosine methyl group due to interactions between ssRNA and dsRNA (Figure S3). Horizontal traces through the ^{13}C positions of the dsRNA and ssRNA resonances are shown in black, blue and cyan, in the bottom panels. Spectra in 'Buffer' and 'Dilute' panels are plotted at the same contour levels, while the spectrum in the 'Condensed' panel is plotted at a higher contour level. All measurements were performed in a buffer comprising 10 mM sodium phosphate, 200 mM NaCl, pH 7.0, 10% D_2O, at 57.5 °C, 800MHz. The concentration of the RNA in buffer was 100 μM.

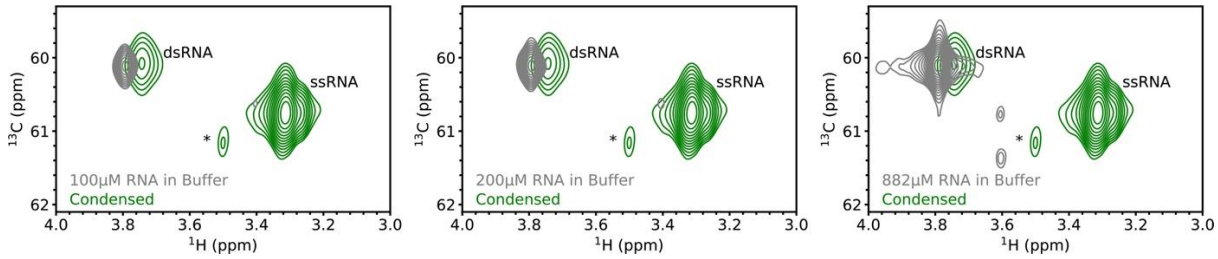

Figure S3. Overlay of [^{13}C,^{1}H] ddHMQC spectra of the RNA methyl region of the condensed phase sample (green) and samples in buffer (gray) at concentrations of 100 μM (left), 200 μM (middle) and 882 μM (right). Several ssRNA peaks become observable in buffer samples as the RNA concentration is increased, consistent with the minor peak in the condensed phase (*) arising from interactions between ssRNA and dsRNA. All measurements were performed in 10mM sodium phosphate, 200mM NaCl, pH 7.0, 10% D_2O at 57.5 °C and 800 MHz.

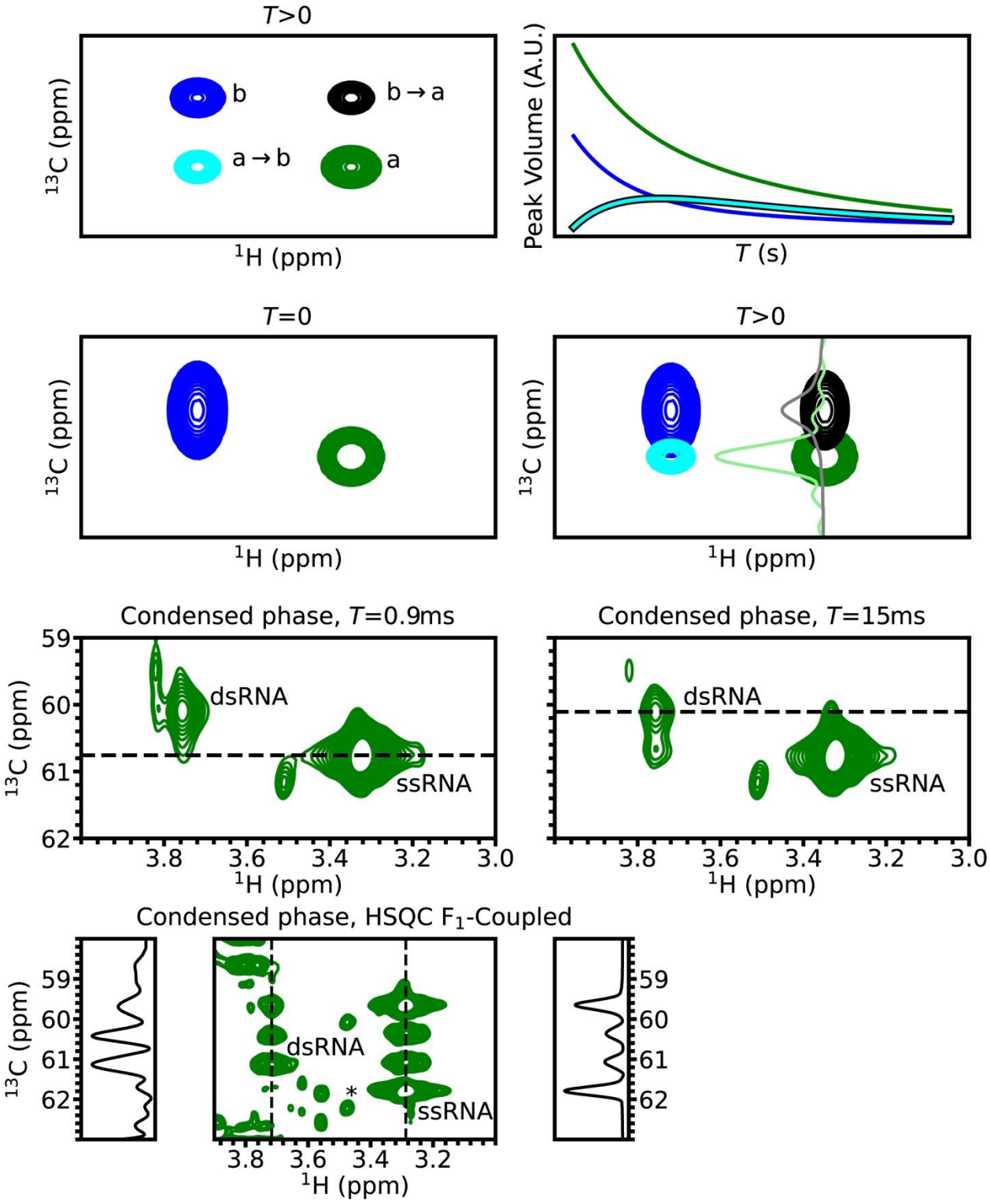

Figure S4. (A) (left) Schematic representation of a spectrum obtained by recording a magnetization exchange experiment where the exchange block is placed after heteronuclear (^{13}C) chemical shift evolution (t_1), for an exchange time $T > 0$. (right) Variation of volume of the cross and diagonal peaks in magnetization exchange

experiments as a function of *T*; the time dependence can be fit to extract kinetics of interconversion between the assumed two states. The data were generated with $k_{a\text{-}b}$ = 2 s^{-1}, $k_{b\text{-}a}$ = 4 s^{-1}, $R_{1,a}$ = 2 s^{-1}, $R_{1,b}$ = 2 s^{-1}, assuming equilibrium magnetization values at the start of the exchange block. (B) (left) Schematic illustrating complications when diagonal peaks are poorly resolved in the heteronuclear (^{13}C) dimension, with broad (blue) and narrow (green) peaks, as in the present application. (right) In this case, the intensities of the cross-peaks are perturbed by the diagonal peaks, especially for short *T* values, while even slight imperfections in the intense green peak, including sinc wiggles, can modulate the intensity of the blue to green cross-peak (black; traces in light green and gray). In the present application the intensities of cross-peaks are weak as they are attenuated by the rapid relaxation of magnetization during *T*, exacerbating the problem. (C) 2D [^{13}C,^{1}H] ddHMQC-based magnetization exchange spectra recorded on an RNA:CAPRIN1 condensed phase sample, *T*=0.9 ms (left) and *T*=15 ms (right) at 57.5 °C, 800 MHz. The diagonal peaks affect the measured intensities of cross-peaks (dashed lines). (D) 2D [^{13}C,^{1}H] F_1-coupled HSQC spectrum recorded on the condensed phase sample (57.5 °C, 800MHz). Also shown on the left (right) are traces at 2'-O-methyl ^{1}H resonance positions for the dsRNA (ssRNA) (dashed lines). * denotes a minor peak arising from interactions between the ssRNA and dsRNA species (Figure S3). Additional peaks shown in the spectrum derive from natural abundance CAPRIN1 signals.

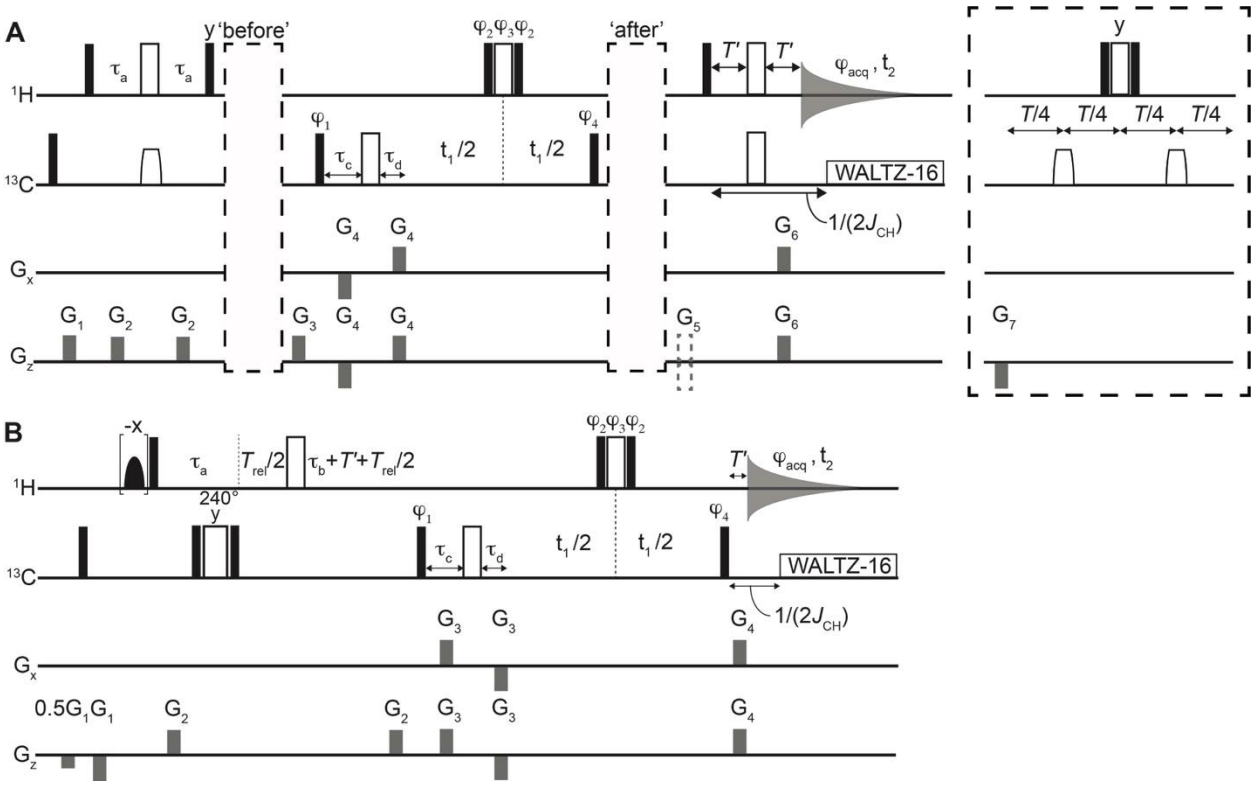

Figure S5. ddHSQC based pulse sequence for measurement of magnetization exchange (A) and ddHMQC based pulse sequence for measurement of effective ^{1}H transverse relaxation rates (T_2) (B) in condensed phase RNA samples. Although ^{1}H transverse relaxation in a methyl group is not single exponential[24], only short values of relaxation times are considered here so that the decay constant measured is an effective average over different rates. Narrow black (wide white) rectangular bars denote non-selective 90° (180°) pulses applied along the x axis unless specified otherwise. (A) Open white trapezoidal shaped pulses are adiabatic (400 μs, 80 kHz sweep). The exchange block (T; dashed box at right hand side of the figure), in which cross-correlation between ^{1}H-^{13}C dipole and ^{13}C/^{1}H CSA interactions are suppressed[25-26], is placed either before or after the t_1 period, inserted into the box labeled as 'before' or 'after'. Delays used are as follows: τ_a is optimized on a per-sample basis for maximum sensitivity and is typically less than $1/(2J_{CH})$, where J_{CH} = 144 Hz for a 2'-O-CH_3 methyl in RNA; $\tau_c = G_4$ + 2 x pwh180 where G_4 is the sum of durations of the gradient and gradient recovery period (typically 200 μs) that follows, and pwh180 is the duration of a ^{1}H 180° pulse; $\tau_d = G_4$ and T' = 500 μs (time for gradient G_6 and subsequent 200 μs delay). The duration 2 x pwh180 is added to τ_c to compensate for the ^{13}C chemical shift evolution that occurs due to the finite length of the composite ^{1}H 180° pulse. A modified WALTZ-16 decoupling scheme is applied at a time $1/(2J_{CH})$ after the last ^{1}H 90° pulse as described previously[8]. The sign of the gradient G_5 (dashed gradient) is positive when the ZZ exchange block is placed after t_1 and negative when the ZZ exchange block is placed before t_1 to minimize the signal from

water. Quadrature in F_1 is achieved by recording a pair of FIDs for each t_1 point with the sign of gradient G_6 inverted. The phase cycle used is: φ_1 = x,-x; φ_2 = 4(x), 4(-x), φ_3 = 4(y), 4(-y), φ_4 = 2(x),2(-x), φ_{acq} = x,2(-x),x. Gradient strengths and durations are G_1=(30%, 0.5 ms), G_2=(25%, 0.3 ms), G_3=(50%, 0.256 ms), G_4=(80%, 0.256 ms), G_5('before') =(-30%, 0.256 ms) and G_5('after')=(30%, 0.256 ms), G_6=(40%, 0.256 ms) and G_7=(-50%, 0.1 ms). The experiment is recorded as a pseudo-4D data set, wherein FIDs in which the ZZ exchange block is placed after and before t_1 are collected in an interleaved manner.

(B) The black shaped pulse is selective for water and ensures that water magnetization is placed along the z-axis prior to t_2 acquisition, at least in the limit of relatively short t_1 times. It is not used in this case, as the ^{1}H resonance position of the 2'-O-CH_3 sugar methyl protons in RNA is close to water. The delay $\tau_a + \tau_b + T'$ is optimized on a per-sample basis for maximum sensitivity and is typically less than $1/(2J_{CH})$, where J_{CH} = 144 Hz for a 2'-O-CH_3 methyl in RNA; $\tau_b = \tau_a - 2G_3$ - pwc180 + 2 x pwh180 where G_3 is the sum of durations of the gradient and gradient recovery period (typically 200 μs); $\tau_c = G_3$; $\tau_d = G_3$ – 2 x pwh180, T' = 500 μs (time for gradient G_4 and subsequent 200 μs delay) and T_{rel} is the relaxation delay. A modified WALTZ-16 decoupling scheme is applied at a time $1/(2J_{CH})$ after the last ^{13}C 90° pulse of phase φ_4 as described previously[8]. Quadrature in F_1 is achieved by recording a pair of FIDs for each t_1 point with the sign of gradient G_3 inverted. The phase cycle used is: φ_1 = x,-x; φ_2 = 2(x),2(y); φ_3 = 2(y),2(-x); φ_4 = 4(x),4(-x); φ_{acq} = x,2(-x),x,-x,2(x),-x. Gradient strengths and durations are G_1=(-25%, 1 ms), G_2=(30%, 0.5 ms), G_3=(80%, 0.256 ms) and G_4=(40%, 0.256 ms). The T_2 experiment is recorded as a pseudo-3D data set, with the relaxation delays recorded in an interleaved manner (i.e., prior to incrementation of t_1).

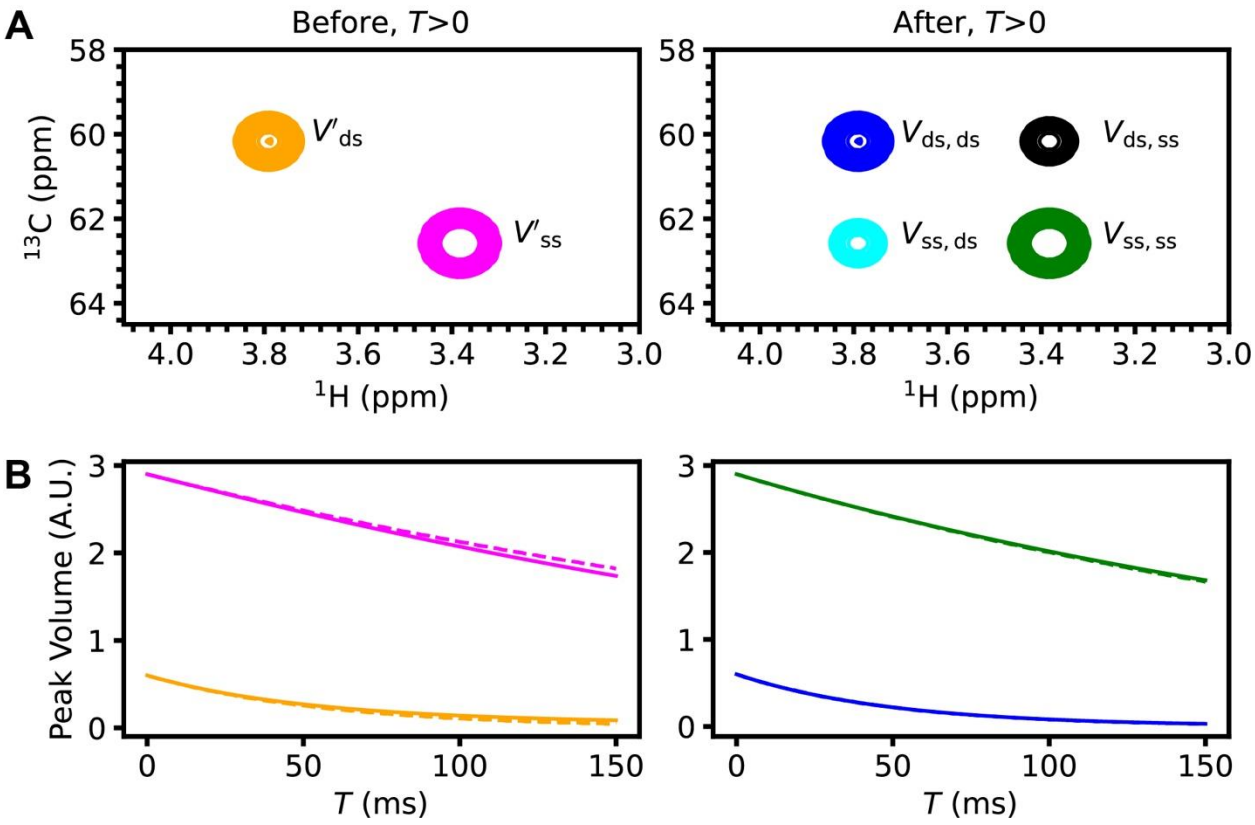

Figure S6. (A) Schematic representation of spectra obtained from magnetization exchange experiments in which the exchange block (T) is placed before t_1 (left) and after t_1 (right). (B) Schematic representation of variation of the peak volumes (solid lines) of the diagonal peaks in the before (left) and after (right) experiments as function of exchange time (T). Also shown in dashed lines are short delay time limit exponential decays for the respective diagonal peaks (see 'Measuring exchange parameters by analysis of diagonal peak intensities'). Exchange parameters used for these calculations were those obtained from fits of the condensed phase experimental data (Table S1; $k_{ss\text{-}ds}$=0.6 s^{-1}, $k_{ds\text{-}ss}$=2.9s^{-1}, $R_{1zz,ds}$=17.2s^{-1}, $R_{1zz,ss}$=3.1s^{-1}) and it was assumed that the 'amount' of longitudinal order for each species immediately prior to the exchange blocks was that expected for a system in equilibrium.

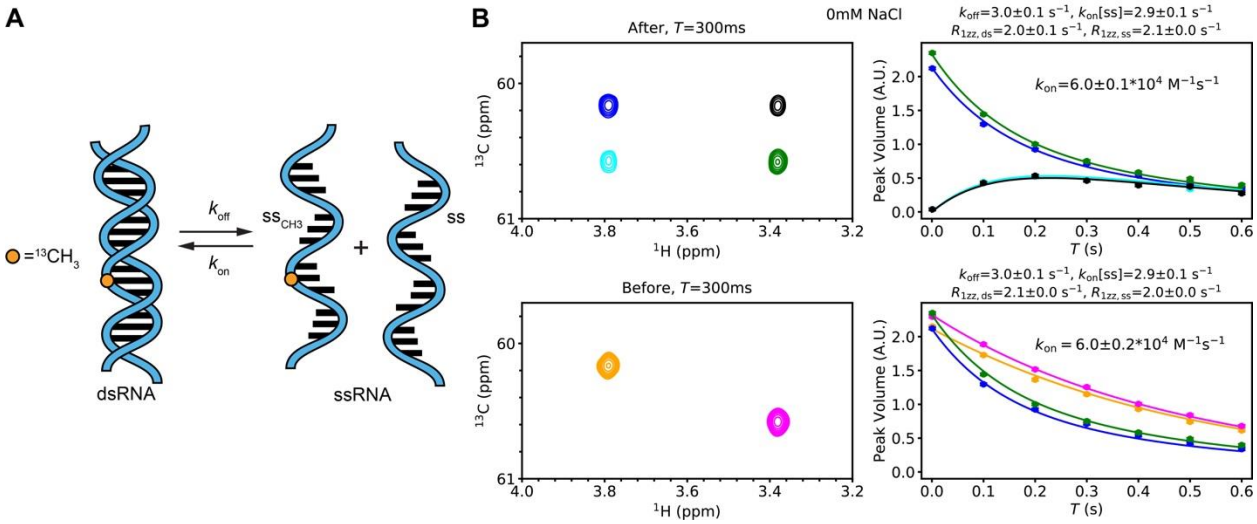

Figure S7. (A) Schematic representation of the ssRNA-dsRNA equilibrium. The 2'-O-methyl group probe is denoted by an orange circle. (B) 2D [^{13}C,^{1}H] ddHSQC-based magnetization exchange spectra recorded on an RNA sample in buffer, T=300 ms, where the exchange block is placed after (top, left) or before (bottom, left) t_1. Cross and diagonal peaks are color coded. Variation of volumes (circles) of the cross and diagonal peaks in the 'after' experiment (top right), and diagonal peaks in the 'before' and 'after' experiments (bottom right) as function of exchange time T. Solid lines denote fits of the data to Eqs. [S2-S3] (top right) and Eqs. [S2-S5] (bottom right). Error bars for the data points were obtained from duplicate experiments, and those for the exchange parameters were obtained using a Monte-Carlo procedure, as described in Materials and Methods. All measurements were performed on a sample of methyl labeled RNA (100μM, Figure 1A) in 10mM sodium phosphate, 10% D_2O, pH 7.0 at 57.5 °C, 800 MHz.

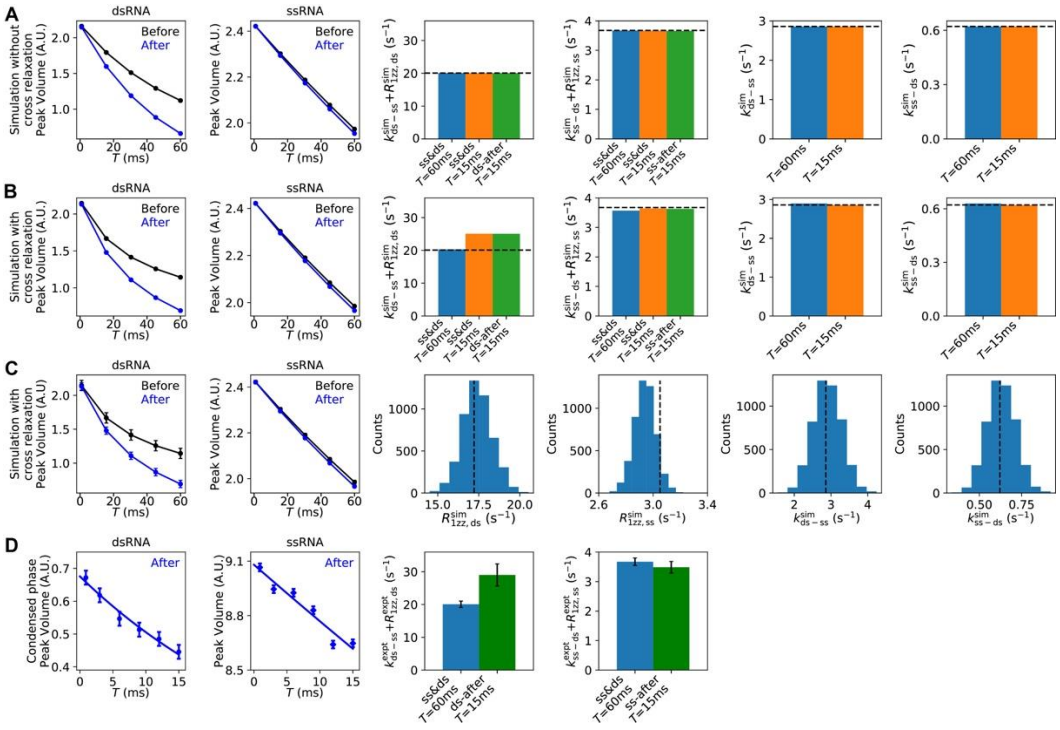

Figure S8. Evaluation of the effects of cross relaxation on the extraction of kinetic rates. First two columns show simulated data (points) in the absence of cross relaxation (A), in the presence of cross relaxation, without (B) and with (C), error, and (D) experimental data recorded on the condensed phase in the 'after' experiment. Solid curves in A-C are not fits, but intended to guide the eye, while the solid curve in D is derived from a fit of the data to an exponential decay function. The third to sixth columns in A and B show exchange parameters obtained from fits of the data in the first two panels to Eqs. [S2-S5] using simulated time dependent volumes of ssRNA and dsRNA diagonal peaks for *T*=60ms (blue) and *T*=15ms (orange); parameters from exponential fits of the 'after' diagonal data, extending to *T*=15ms, are shown in green for dsRNA (ds-after, *T*=15ms) and ssRNA (ss-after, *T*=15ms). Histograms of the fitted parameters from analysis of the time dependencies of ssRNA and dsRNA diagonal peaks for *T*=60ms (blue) obtained by fitting simulated data generated with cross relaxation and including errors are shown in C (columns 3-6). Dashed horizontal lines (A-C) denote the values obtained from fits of experimental condensed phase data (Table S1). Exchange parameters used for simulations (A-C) were obtained as described herein (see 'Measuring exchange parameters by analysis of diagonal peak intensities') with errors in C and D (first two columns) obtained as described in Materials and Methods. Error bars in the 3rd and 4th columns of D were obtained using a Monte-Carlo procedure as described in Materials and Methods.

ddHSQC based pulse sequence for measurement of magnetization exchange

/* hsqc_800_lek_deldecW_ZZ_4D_cp

Used to record 13C 1H HSQC, with options for 15N, 13C and 2H decoupling during t1

Written by LEK and RM on Nov 26

Modified by LEK on Feb 12, 2015 to correct GRAMP/GRAD issue

Modified by LEK on July 19, 2016 to include coherence transfer gradients
that are useful when using ddx4 samples where only a small fraction of
material is 13C labeled

Modified by LEK on April 26 to ensure that gradients do not interfer with 15N decoupling

Delayed decouping HSQC !! (not hmqc) with coherence transfer gradients - USED for CAPRIN1 samples
if no CAPRIN1 then dont use coherence transfer; written by LEK on Dec 4, 2023

This experiment allows one to record magnetization exchange on a sample in condensed phase for example

Modified by LEK on Dec 22, 2023 to allow for 13C decoupling during the initial inept to suppress transfer
of magnetization from 1H to 13C for interferring peaks, -DC_dec

Modified by LEK on Dec 22, 2023 to allow for measurement of T1ZZ either before (-DT1_before) or after

Modified by LEK on Jan 29, 2024 to place the gradient selection after t1
Modified by LEK on Feb 2 to make into a 4D using l3 = 0 (after) or 1 (before)

Modified by LEK on March 7, 2024 to correct an issue with phasing in F2 in the after plane (put gradient after ZZ time)
also moved the coherence transfer gradients in C to before t1

Modified by LEK on March 8, 2024 to correct artifacts caused by 1H 180 in middle of t1. Has some 90o character, which
brings Iz to Ix, so need a gradient immediately after the 13C90o phi5. Alternatlively can phase cycle the 1H 180o x,-x
in middle of t1

```
*/

#include <Avance.incl>
#include <Grad.incl>
#include <Delay.incl>

;Define phases
#define zero ph=0.0
#define one ph=90.0
#define two ph=180.0
#define three ph=270.0

;Define Pulses
define pulse pwh
    "pwh=p1"          ; 1H hard pulse at power pl1
define pulse pwc
    "pwc=p2"          ; 13C hard pulse at power pl2

#if !defined(C_dec) || defined(cross_corr)
define pulse pwc_ad       ; adiabatic pulse for inept transfers
    "pwc_ad = p23"
#endif

define pulse pwc_reb      ; reburp pulse for gradients during t1
    "pwc_reb = p24"
define pulse pwd
    "pwd=p4"          ; 2H pulse at power pl4

;Define delays

"in0=inf1/2"
"d11=30m"

define delay taua
    "taua=d5"         ; < 1/(4JCH) 1.8 ms

define delay tau1

define delay hscuba
 "hscuba=30m"

define list<delay> time_relax = <$VDLIST>

;define flags
```

```
;f1180    ; set zgoptns -Df1180

#ifdef f1180
 "d0=(in0)/2"
#else
 "d0=(0.2u)/2"
#endif

#ifdef OneDarray
#else
define loopcounter ni
 "ni=td1/2"
#endif

;Ndec    ; set zgoptns -DNdec
;COdec   ; set zgoptns -DCOdec
;Ddec    ; set zgoptns -DDdec

/* Assign cnsts to check validity of parameter changes */
#ifdef fsat
  "cnst10 = plw10" ; tsatpwr - set to max of 0.00005W
#endif
  "cnst21=plw21" ; dpwr pl21 - set max at 4.5W
#ifdef COdec
  "cnst22=plw22" ; dpwrco pl22/sw22 - set max at 8.0W
#endif

#if !defined(C_dec) || defined(cross_corr)
  "cnst23=spw23" ; adiabatic 13C pulse
#endif

  "cnst24=spw24" ; reburp 13C pulse

#ifdef Ndec
  "cnst31=plw31" ; dpwr2 pl31 - set max at 5.8W
#endif

#ifdef Ddec
  "cnst4=plw4"   ; dpwr3 pl4 - set max at 10.5W
  "cnst41=plw41" ; dpwr3D pl41 - set max at 1.5W
#endif

; "acqt0=0"  ; select 'DIGIMOD = baseopt' to execute
```

```
; "d20=2u"  Change if you do not want delayed decoupling
"d20 = 1s/(cnst25*2.0) - 1.0m"  ; cnst25 is J_methyl

"l2=0"  ; counter for delays
"l3=0"  ; counter for before (1) or after (0)

1 ze

; check validity of parameters

#ifdef fsat
 if "cnst10 > 0.001"
 {
  2u
  print "error: presat power pl10 is too large"
  goto HaltAcqu
 }
#endif

 if " cnst21 > 6.0"
 {
  2u
  print "error: dpwr pl21 too large"
  goto HaltAcqu
 }

#ifdef COdec
 if " cnst22 > 1.0"
 {
  2u
  print "error: dpwrco pl22 too large"
  goto HaltAcqu
 }
#endif

#if !defined(C_dec) || defined(cross_corr)
 if " cnst23 > 71.0"
 {
  2u
  print "error: power for adiabatic 13C 180 is too large"
  goto HaltAcqu
 }
#endif
```

```
if "pwc_reb > 30u" {
 if " cnst24 > 80.0"
 {
  2u
  print "error: power for reburp 13C 180 is too large"
  goto HaltAcqu
 }
}

#ifdef Ndec
 if " cnst31 > 4.0"
 {
  2u
  print "error: dpwr2 pl31 too large"
  goto HaltAcqu
 }
#endif

 if "pwc > 20u"
 {
  2u
  print "error: pwc too large < 20 us"
  goto HaltAcqu
 }

 if "pwc_reb > 2m"
 {
  2u
  print "error: pwc_reb too large < 2m"
  goto HaltAcqu
 }

#if !defined(C_dec) || defined(cross_corr)
 if "pwc_ad > 500u"
 {
  2u
  print "error: pwc_ad too large < 500 us"
  goto HaltAcqu
 }
#endif

#ifdef Ddec
 if "cnst4 > 15.5"
 {
```

```
  2u
  print "error: dpwr3 pl4 too large"
  goto HaltAcqu
 }

 if "cnst41 > 4.0"
 {
  2u
  print "error: dpwr3D pl41 too large"
  goto HaltAcqu
 }

;   d11 LOCKDEC_ON ; Not required for AvanceIII-HD
  50u LOCKH_ON
  d11 H2_PULSE
  2u pl41:f4     ; set power pl4 for 2H flipback pulses
#endif

2 d11 do:f2

#ifdef Ddec    /* D decoupling */
d11 H2_LOCK    ; put lock channel in lock mode
6m LOCKH_OFF   ; turn off lock hold

#ifdef fsat                    /* zgoptn -Dfsat */
  4u pl10:f1                    ; power(tsatpwr) for presaturation
  d1 cw:f1 zero                   ; Hcw(d1)x
  4u do:f1                      ; cw off
  2u pl1:f1                     ; power(tpwr)

#ifdef fscuba                 /* Scuba pulse sequence */
   hscuba                     ; delay(hscuba)
    (pwh zero):f1               ; H 90x180y90x
    (pwh*2 one):f1
    (pwh zero):f1
   hscuba                     ; delay(hscuba)
#endif                      /* end fscuba */

#else                       /* if fsat is no */
 2u pl1:f1                    ; power(tpwr)
 d1                         ; delay(d1)
#endif                       /* end if fsat */

50u  LOCKH_ON
```

```
15u H2_PULSE

#else   /* no D decoupling */

#ifdef fsat                  /* zgoptn -Dfsat */
 4u pl10:f1                   ; power(tsatpwr) for presaturation
 d1 cw:f1 zero                  ; Hcw(d1)x
 4u do:f1                    ; cw off
 2u pl1:f1                   ; power(tpwr)

#ifdef fscuba               /* Scuba pulse sequence */
  hscuba                    ; delay(hscuba)
   (pwh zero):f1              ; H 90x180y90x
   (pwh*2 one):f1
   (pwh zero):f1
  hscuba                     ; delay(hscuba)
#endif                      /* end fscuba */

#else                       /* if fsat is no */
 2u pl1:f1                    ; power(tpwr)
 d1                         ; delay(d1)
#endif                       /* end if fsat */
#endif                       /* end of D_decoupling */

 2u pl1:f1
 2u pl2:f2
 2u pl31:f3

#ifdef Ddec
 20u UNBLKGRAMP        ; dly 20u, unblank gradients
#else
 20u UNBLKGRAD         ; dly 20u, unblank gradients and lock on hold
#endif

 (pwc zero):f2   ; C90x - To destroy 13C Boltzman magnetization

 2u
 (p50:gp0)      ; gradient 0
 d16

; This is the real start

"tau1 = d0"
```

```
if "tau1 < 0.2u" {
  "tau1 = 0.2u"
}

#ifndef C_dec

 (pwh zero):f1                    ; H90x

 2u
 p51:gp1                         ; gradient 1
 d16

 "DELTA = taua - 2.0u - p51 - d16 - pwc_ad*0.5"
 DELTA                           ; delay 1/4JCH

 (center(pwh*2 ph26):f1 (pwc_ad:sp23 ph26):f2)  ; H180x,C180x

 "DELTA = taua - 2.0u - p51 - d16 - pwc_ad*0.5"
 DELTA                           ; delay 1/4JCH

 2u
 p51:gp1                         ; gradient 1
 d16

 (pwh one):f1                    ; H90y

#else
 (pwh zero):f1                    ; H90x

 2u pl27:f2   ; reset power for decoupling
 (taua cpd7 ph26):f2
 2u do:f2
 2u pl2:f2

 (center(pwh*2 ph26):f1 (pwc*2.0 ph26):f2)  ; H180x,C180x

 2u pl27:f2   ; reset power for decoupling
 (taua cpd7 ph26):f2
 2u do:f2
 2u pl2:f2
 (pwh one):f1                    ; H90y
#endif

if "l3 % 2 ==  1" {
```

```
#ifndef cross_corr

 2u gron7        ; positive
 100u
 100u groff

 "DELTA = time_relax[l2]"   ; zz exchange for a net time of time_relax
  DELTA

#else

 2u gron8        ; negative
 100u
 100u groff

 "DELTA = time_relax[l2]/4.0 - pwc_ad*0.5"   ; zz exchange for a net time of time_relax
 1u
 "DELTA1 = time_relax[l2]/4.0 - pwc_ad*0.5 - pwh*2.0"    ; zz exchange for a net time of
time_relax
 DELTA
 (pwc_ad:sp23 ph26):f2
 DELTA1
 (pwh ph26 pwh*2.0 ph27 pwh ph26):f1
 DELTA1
 (pwc_ad:sp23 ph26):f2
  DELTA pl2:f2

#endif
}

 2u
 p52:gp2    ; must be positive gradient
 100u

/*  If zgoptn -DDdec turn on 2H dec */

# ifdef Ddec
 2u pl4:f4          ; dly 2u,  set pwr pl4 dpwr3
 (pwd one):f4        ; 2H 90(y)
 2u pl41:f4         ; dly 2u,  set pwr pl41 dpwr3D
 (2u cpd4 zero):f4    ; Turn on 2H decoupling - cpd4, phase x
# endif
```

```
/*  If zgoptn -DNdec turn on 15N dec */
# ifdef Ndec
 2u pl31:f3   ; set power pl31 for 15N decoupling
 (2u cpds3 ph26):f3  ; Turn on 15N decoupling, cpdprg3 - waltz16
# endif

 2u pl2:f2
 (pwc ph3):f2                    ; C90ph3

 2u
 p55:gp5*-1.0                ; coherence transfer gradient 5
"DELTA = d16 + 2u + 2u + pwh + 1u + pwh*2 + 1u + pwh + 2u + 2u + 2u + 2u + 2u"
 DELTA

 (pwc_reb:sp24 ph26):f2  ; reburp C180x

 2u
 p55:gp5                  ; coherence transfer gradient 5
 d16

/* If zgoptn -DCOdec turn on off-resonance CO dec */

# ifdef COdec
 2u pl22:f2
 (2u cpds8 ph26):f2  ; Turn on CO dec, cpdprg8, sync mode
# else
 2u
 2u
#endif

 tau1                    ; t1/2

 (pwh ph6):f1
 1u
 (pwh*2 ph7):f1
 1u
 (pwh ph6):f1

  tau1

# ifdef COdec
 2u do:f2   ; Turn off CO decoupling
 2u pl2:f2  ; set 13C high power
#else
```

```
 2u
 2u
# endif

# ifdef Ndec
 2u
 2u do:f3    ; Turn off 15N decoupling on channel 3
#else
 2u
 2u
# endif

 2u pl2:f2
 (pwc ph5):f2              ; C90ph5

# ifdef Ddec
 2u do:f4           ; Turn off 2H decoupling on channel 4
 2u pl4:f4          ; dly 2u,  set pwr pl4 dpwr3
 (pwd three):f4       ; 2H 90(-y)
# endif


if "l3 %2 == 0"
{

#ifndef cross_corr
 2u gron8
 100u
 100u groff

 "DELTA = time_relax[l2]"   ; zz exchange for a net time of time_relax
  DELTA

 2u
 p53:gp3                  ; gradient 3
 100u
#else
 2u gron8
 100u
 100u groff

 "DELTA = time_relax[l2]/4.0 - pwc_ad*0.5"   ; zz exchange for a net time of time_relax
 1u
```

```
 "DELTA1 = time_relax[l2]/4.0 - pwc_ad*0.5 - pwh*2.0"    ; zz exchange for a net time of time_relax
 DELTA
 (pwc_ad:sp23 ph26):f2
 DELTA1
 (pwh ph26 pwh*2.0 ph27 pwh ph26):f1
 DELTA1
 (pwc_ad:sp23 ph26):f2
  DELTA pl2:f2

 2u
 p53:gp3*-1.0   ; p53 is negative
 100u
#endif
}

0.2u

if "l3 %2 == 1" {
 2u
 p53:gp3                ; gradient 3
 100u
}

1u

 (pwh zero):f1              ; H90x

 "DELTA = 0.5m - pwh*2.0/PI + de"
 DELTA                          ; delay 1/4JCH

 (center(pwh*2 ph26):f1 (pwc*2.0 ph26):f2)  ; H180x,C180x

 "DELTA = 0.5m - 2u - p56 - d16 - 4u - 2u"
 DELTA                          ; delay 1/4JCH

 2u
 p56:gp6*EA                     ; gradient 6 CHT
 d16

#ifdef Ddec
 4u BLKGRAMP
#else
 4u BLKGRAD
```

```
#endif

 2u pl21:f2            ; lower power for 13C decoupling

 go=2 ph31 cpds2:f2       ; acquire fid with syncronous 13C decoupling during aq
 d11 do:f2 mc #0 to 2
 F3QF(calclc(l3,1))
 F2QF(calclc(l2,1))
 F1EA(calgrad(EA),calph(ph3,+180) & calph(ph31, +180) & caldel(d0, +in0))

#ifdef Ddec
d11 H2_LOCK
d11 LOCKH_OFF
; d11 LOCKDEC_OFF ; use statement for earlier hardware
#endif

HaltAcqu, 1m
exit

ph3=0 2
ph5=0 0 2 2
ph6=0 0 0 0 2 2 2 2
ph7=1 1 1 1 3 3 3 3
ph31=0 2 2 0
ph26=0
ph27=1
ph28=2
ph29=3

;d1 : repetition delay
;d5 : 2*taua is the optimum transfer time based on the measured R2s
;d11 : delay for disk i/o, 30ms
;d16 : gradient recovery delay, 200us
;pl1 : tpwr - power level for pwh
;pl2 : dhpwr - power level for hard 13C pulse pwc
;pl21 : dpwr - power level for  13C decoupling cpd2
;pl22 : dpwrcodec - power level for cos modulated seduce
;pl27 : power level for C decoupling during inept
;sp22 : cos modulated seduce decoupling pattern
;sp23 : power level for pwc_ad
;p23  : pwc_ad - adiabatic pulses for INEPT transfer
;p24  : pwc_reb - reburp pulses during t1
;pl31 : dpwr2 - power level for 15N cpd3
;pl4 : dpwr3 - power level for 2H flipback pulses
```

;pl41 : dpwr3D - power level for 2H cpd4
;p1 : pwh
;p2 : pwc
;p22 : pwco90 (seduce1 dec) pattern length us @ pl22 for CO decoupling
;p27 : Length of decoupling element during first INEPT
;p31 : pwn at dpwr2 for 15N decoupling during 2*TC(~29ms)
;p4 : pwd at dpwr3 for 2H flipback pulses
;p41 : pwddec at dpwr3D for 2H decoupling
;ni : td1/2 number of complex points in t1
;cpd2 : 13C decoupling according to program defined by cpdprg2
;cpd3 : 15N decoupling according to program defined by cpdprg3
;cpd4 : 2H decoupling according to program defined by cpdprg4
;cpd8 : 13CO decoupling according to program defined by cpdprg8
;pcpd2: 13C 90 degree pulse at pl21 for cpd2
;pcpd3: 15N 90 degree pulse at pl31 for cpd3
;pcpd4: 2H 90 degree pulse at pl41 for cpd4
;pcpd8: seduce1 decoupling pattern length for cpd8
;spnam22 : file name for CO decoupling
;spnam23 : file name for chirp pulse during inepts
;spnam24 : file name for reburp pulse during t1
;cnst25 : actual JCH value 125Hz for ILV 143 Hz for CH3-O-sugar
;cpdprg7 : C decoupling during first INEPT
;zgoptns :Df1180,DNdec,DCOdec,DDdec,Dfsat,DOneDarray,Dfscuba,DC_dec,Dcross_corr

ddHMQC based pulse sequence for measurement of ^1H T_2

```
/* hmqc_lek_800_delaydecW_HT2_cp

 Used to record 13C 1H HMQC of methyl groups, with options for 15N, 13C and 2H decoupling during t1
 Use for D2O samples and 15N,13C decoupling turned off
  spectrum to be reconstructed using machine learning - collaboration with DFH
 Used adiabatic bilevel decopuling contructed with C13_wu_anti.par and C13_wu_antii.par
  set power for both bi-levels to be 3 dB more than what wavemaker gives

 Use ns=4 with current version of decoupling which has ns%4

 Written by LEK

 Modified by LEK on Dec 9, 2022 to include a double buffer flag for some of Alex's work

 Modified by LEK on Jan 19, 2022 to enable recording of spectra in water - uses gradients for coherence transfer

!   sit on water   !

 Preferred version.

 2*taua - p52 - d16 - p52 - d16 + BigT = '1/(2J)'
 2*taua - 412u = '1/(2J)'

 Modified by LEK on Feb 28, 2022 to change C 180 during inept to 90x240y90x

 June 16, 2023, modified by LEK to include xy phase cycle of 1H 180 in t1 period

 Modified by LEK on Nov 24, 2023 to account for the fact that J values can be different for
  different methyls. ILV - 125 Hz. M - 140 Hz. CH3-O-Sugar(RNA) - 142 Hz.
  Use parameter cnst25 = J_methyl

 This pulse sequence allows measurement of the 1H T2 for correction of peak intensities due to
  relaxation - time_relax

*/
```

```
#include <Avance.incl>
#include <Grad.incl>
#include <Delay.incl>

;Define phases
#define zero ph=0.0
#define one ph=90.0
#define two ph=180.0
#define three ph=270.0

;Define Pulses
define pulse pwh
    "pwh=p1"          ; 1H hard pulse at power pl1
define pulse pw_sl1
    "pw_sl1=p14"      ; eburp1 pulse
define pulse pw_sl11
    "pw_sl11=p15"     ; seduce water pulse at the start, on resonance
define pulse pwc
    "pwc=p2"          ; 13C hard pulse at power pl2

"in0=inf1/2"
"d11=30m"

define delay taua
    "taua=d5"         ; < 1/(4JCH) 1.8 ms

define delay tau1

define delay hscuba
 "hscuba=30m"

define delay Big_T
  "Big_T=d6"  ; set to 0.5 ms

;define flags
;f1180    ; set zgoptns -Df1180

#ifdef f1180
 "d0=(in0)/2"
#else
 "d0=(0.2u)/2"
#endif
```

```
#ifdef OneDarray
#else
define loopcounter ni
 "ni=td1/2"
#endif

define list<delay> time_relax = <$VDLIST>

/* Assign cnsts to check validity of parameter changes */
#ifdef fsat
  "cnst10 = plw10" ; tsatpwr - set to max of 0.00005W
#endif

#ifdef buffer_flg
  "cnst14=spw14" ; power level for eburp1 pulse for buffer_flg
#endif

  "cnst15=spw15" ; power level for seduce pulse preeceding start of sequence

  "cnst21=plw21" ; dpwr pl21 - set max at 4.5W

"d20 = 1s/(cnst25*2.0) - Big_T"  ; cnst25 is J_methyl

"l3 = 0" ; loop counter to increment the vd list

1 ze

; check validity of parameters

 if "aq > 0.100"
 {
  2u
  print "error: aq is too large <= 100 ms"
  goto HaltAcqu
 }

#ifdef fsat
 if "cnst10 > 0.001"
 {
  2u
  print "error: presat power pl10 is too large"
  goto HaltAcqu
 }
#endif
```

```
#ifdef buffer_flg
 if "cnst14 > 0.015"
 {
  2u
  print "error: power level for eburp1 pulse is too large"
  goto HaltAcqu
 }
#endif

 if "cnst15 > 0.015"
 {
  2u
  print "error: power level for seduce water pulse at start is too large"
  goto HaltAcqu
 }

 if " cnst21 > 6.5"
 {
  2u
  print "error: 13C dec power is too large"
  goto HaltAcqu
 }

 if "pwc > 20u"
 {
  2u
  print "error: pwc too large < 20 us"
  goto HaltAcqu
 }

2 d11 do:f2

 20u fq=0:f1              ; sit on water

#ifdef fsat                /* zgoptn -Dfsat */
 4u pl10:f1                ; power(tsatpwr) for presaturation
 d1 cw:f1 zero               ; Hcw(d1)x
 4u do:f1                  ; cw off
 2u pl1:f1                 ; power(tpwr)

#ifdef fscuba             /* Scuba pulse sequence */
  hscuba                 ; delay(hscuba)
   (pwh zero):f1            ; H 90x180y90x
```

```
   (pwh*2 one):f1
   (pwh zero):f1
  hscuba                ; delay(hscuba)
#endif                  /* end fscuba */

#else                   /* if fsat is no */
 2u pl1:f1              ; power(tpwr)
 d1                     ; delay(d1)
#endif                  /* end if fsat */

 20u UNBLKGRAD          ; dly 20u, unblank gradients and lock hold

 2u
 p50:gp0*0.5     ; gradient 0*0.5
 d16

#ifdef buffer_flg
#ifdef doubl_buff

 20u fq=cnst23:f1           ; jump from water to second buffer position
 2u
 (pw_sl1:sp14 zero):f1
 2u

 2u
 (p53:gp3)     ; gradient 3
 d16
#endif
 20u fq=cnst2:f1            ; jump from water to first buffer position
 2u
 (pw_sl1:sp14 zero):f1
 2u
#endif

 10u fq=0:f1                ; jump back to water
 2u pl1:f1
 2u pl2:f2
 2u pl31:f3

 (pwc zero):f2   ; C90x - To destroy 13C Boltzman magnetization

 2u
 (p50:gp0)     ; gradient 0
 d16
```

```
; This is the real start

"tau1 = d0"

if "tau1 < 0.2u" {
  "tau1 = 0.2u"
}

 "DELTA1 = time_relax[l3]"

 2u

 "DELTA2 = DELTA1/2.0"

 2u
 (pw_sl11:sp15 ph28):f1
 2u pl1:f1

 (pwh ph26):f1                    ; H90x

 2u
 p51:gp1
 d16

"DELTA = taua - 2.0u - p51 - d16 - pwh*2.0/PI - pwc*4.666 - 1u - 1u"
 DELTA

 (pwc ph26 1u pwc*2.666 ph27 1u pwc ph26):f2

DELTA2

 (pwh*2.0 ph26):f1

 "DELTA = taua - 2u - p51 - d16 - 2u - p52 - d16 - pwc*2 - 2u - p52 - d16 + Big_T + pwh + 2u +
pwh*2 + 2u + pwh + de + 4u + 2u + DELTA2"
 DELTA

 2u
 p51:gp1
 d16

 (pwc ph3):f2                     ; C90ph3
```

```
 2u
 p52:gp2*EA                    ; gradient 2, coherence transfer
 d16

 (pwc*2.0 ph26):f2

 2u
 p52:gp2*EA*-1.0               ; gradient 2, coherence transfer
"DELTA = d16 - pwh - 2u - pwh*2 - 2u - pwh"
 DELTA

 tau1                  ; t1/2

 (pwh ph5):f1          ; H90x
 2u
 (pwh*2 ph6):f1        ; H180y
 2u
 (pwh ph5):f1          ; H90x

  tau1

 (pwc ph8):f2          ; C90 ph8

 "DELTA = Big_T - 2u - p54 - d16"
  DELTA

 2u
 p54:gp4               ; gradient 4, coherence transfer
 d16

 4u BLKGRAD

 2u pl21:f2          ; lower power for 13C decoupling

 go=2 ph31 cpds2:f2    ; acquire fid with delayed 13C decoupling
 d11 do:f2 mc #0 to 2
 F2QF(calclc(l3,1))
 F1EA(calgrad(EA),calph(ph3,+180) & calph(ph31, +180) & caldel(d0, +in0))

HaltAcqu, 1m
exit

ph3=0 2
ph5=0 0 1 1
```

```
ph6=1 1 2 2
ph8=0 0 0 0 2 2 2 2
ph31=0 2 2 0 2 0 0 2
ph26=0
ph27=1
ph28=2
ph29=3

;d1 : repetition delay
;d5 : taua ; 2*d5 - 0.412 ms = 1/2J ; if taua is normally 1.8 use 2.05- ADJUST
;d6 : time alloted for 1H coherence gradient and recovery; set to .5m
;d11 : delay for disk i/o, 30ms
;d16 : gradient recovery delay, 200us
;d20 : set to exactly 1/2JCH when decoupling begins in t2
;pl1 : tpwr - power level for pwh
;pl2 : dhpwr - power level for hard 13C pulse pwc
;pl21 : dpwr - power level for  13C decoupling cpd2
;spnam14: eburp1 pulse on buffer
;spnam15: seduce pulse on water
;p1 : pwh
;p14 : eburp1 pulse width on buffer, typically 7000u
;p15 : seduce pulse on water (sel 4)
;p2 : pwc
;ni : td1/2 number of complex points in t1
;cpd2 : 13C decoupling according to program defined by cpdprg2
;pcpd2:  13C 90 degree pulse at pl21 for cpd2
;cnst2 :  buffer(Hz) - water(Hz)
;cnst23 : second buffer(Hz) - water(Hz)
;cnst25 : actual JCH value 125Hz for ILV 143 Hz for CH3-O-sugar
;zgoptns : Df1180,Dfsat,DoneDarray,Dfscuba,Dbuffer_flg,Ddoubl_buff
```

References

1. Wong, L. E.; Kim, T. H.; Muhandiram, D. R.; Forman-Kay, J. D.; Kay, L. E., NMR Experiments for Studies of Dilute and Condensed Protein Phases: Application to the Phase-Separating Protein CAPRIN1. *J Am Chem Soc* **2020,** *142* (5), 2471-2489.
2. Toyama, Y.; Rangadurai, A. K.; Forman-Kay, J. D.; Kay, L. E., Mapping the per-residue surface electrostatic potential of CAPRIN1 along its phase-separation trajectory. *Proc Natl Acad Sci U S A* **2022,** *119* (36), e2210492119.
3. Kloiber, K.; Spitzer, R.; Tollinger, M.; Konrat, R.; Kreutz, C., Probing RNA dynamics via longitudinal exchange and CPMG relaxation dispersion NMR spectroscopy using a sensitive 13C-methyl label. *Nucleic Acids Res* **2011,** *39* (10), 4340-51.
4. Strebitzer, E.; Nussbaumer, F.; Kremser, J.; Tollinger, M.; Kreutz, C., Studying sparsely populated conformational states in RNA combining chemical synthesis and solution NMR spectroscopy. *Methods* **2018,** *148*, 39-47.
5. Basanta-Sanchez, M.; Temple, S.; Ansari, S. A.; D'Amico, A.; Agris, P. F., Attomole quantification and global profile of RNA modifications: Epitranscriptome of human neural stem cells. *Nucleic Acids Res* **2016,** *44* (3), e26.
6. Delaglio, F.; Grzesiek, S.; Vuister, G. W.; Zhu, G.; Pfeifer, J.; Bax, A., NMRPipe: a multidimensional spectral processing system based on UNIX pipes. *J Biomol NMR* **1995,** *6* (3), 277-93.
7. Ahmed, R.; Rangadurai, A. K.; Ruetz, L.; Tollinger, M.; Kreutz, C.; Kay, L. E., A delayed decoupling methyl-TROSY pulse sequence for atomic resolution studies of folded proteins and RNAs in condensates. *J Magn Reson* **2024**, 107667.
8. Bolik-Coulon, N.; Sever, A. I. M.; Harkness, R. W.; Aramini, J. M.; Toyama, Y.; Hansen, D. F.; Kay, L. E., Less is more: A simple methyl-TROSY based pulse scheme offers improved sensitivity in applications to high molecular weight complexes. *J Magn Reson* **2023,** *346*, 107326.
9. Choy, W. Y.; Mulder, F. A.; Crowhurst, K. A.; Muhandiram, D. R.; Millett, I. S.; Doniach, S.; Forman-Kay, J. D.; Kay, L. E., Distribution of molecular size within an unfolded state ensemble using small-angle X-ray scattering and pulse field gradient NMR techniques. *J Mol Biol* **2002,** *316* (1), 101-12.
10. Wu, D. H.; Chen, A. D.; Johnson, C. S., An Improved Diffusion-Ordered Spectroscopy Experiment Incorporating Bipolar-Gradient Pulses. *J Magn Reson* **1995,** *115*, 260-264.
11. Huang, R.; Brady, J. P.; Sekhar, A.; Yuwen, T.; Kay, L. E., An enhanced sensitivity methyl (1)H triple-quantum pulse scheme for measuring diffusion constants of macromolecules. *J Biomol NMR* **2017,** *68* (4), 249-255.
12. Hwang, T. L.; Shaka, A. J., Water Suppression That Works. Excitation Sculpting Using Arbitrary Wave-Forms and Pulsed-Field Gradients. *J Magn Reson* **1995,** *112*, 275-279.
13. Toyama, Y.; Rangadurai, A. K.; Forman-Kay, J. D.; Kay, L. E., Surface electrostatics dictate RNA-binding protein CAPRIN1 condensate concentration and hydrodynamic properties. *J Biol Chem* **2023,** *299* (1), 102776.
14. Vetterling, W. T.; Teukolsky, S. A.; Press, W. H.; Flannery, B. P., *Numerical Recipes in C: The Art of Scientific Computing*. Cambridge University Press: 1992.
15. Koehler, E.; Brown, E.; Haneuse, S. J., On the Assessment of Monte Carlo Error in Simulation-Based Statistical Analyses. *Am Stat* **2009,** *63* (2), 155-162.

16. Farrow, N. A.; Zhang, O.; Forman-Kay, J. D.; Kay, L. E., A heteronuclear correlation experiment for simultaneous determination of 15N longitudinal decay and chemical exchange rates of systems in slow equilibrium. *J Biomol NMR* **1994,** *4* (5), 727-34.
17. Montelione, G. T.; Wagner, G., 2D Chemical exchange NMR spectroscopy by proton-detected heteronuclear correlation. *J Am Chem Soc* **1989,** *111*, 3096-3098.
18. Miloushev, V. Z.; Bahna, F.; Ciatto, C.; Ahlsen, G.; Honig, B.; Shapiro, L.; Palmer, A. G., 3rd, Dynamic properties of a type II cadherin adhesive domain: implications for the mechanism of strand-swapping of classical cadherins. *Structure* **2008,** *16* (8), 1195-205.
19. Tollinger, M.; Skrynnikov, N. R.; Mulder, F. A.; Forman-Kay, J. D.; Kay, L. E., Slow dynamics in folded and unfolded states of an SH3 domain. *J Am Chem Soc* **2001,** *123* (46), 11341-52.
20. Religa, T. L.; Sprangers, R.; Kay, L. E., Dynamic regulation of archaeal proteasome gate opening as studied by TROSY NMR. *Science* **2010,** *328* (5974), 98-102.
21. Tugarinov, V.; Scheurer, C.; Bruschweiler, R.; Kay, L. E., Estimates of methyl 13C and 1H CSA values (Dr) in proteins from cross-correlated spin relaxation. *J Biomol NMR* **2004,** *30*, 397-406.
22. Sekhar, A.; Rosenzweig, R.; Bouvignies, G.; Kay, L. E., Hsp70 biases the folding pathways of client proteins. *Proc Natl Acad Sci U S A* **2016,** *113* (20), E2794-801.
23. Yuwen, T.; Sekhar, A.; Kay, L. E., Evaluating the influence of initial magnetization conditions on extracted exchange parameters in NMR relaxation experiments: applications to CPMG and CEST. *J Biomol NMR* **2016,** *65* (3-4), 143-156.
24. Tugarinov, V.; Hwang, P. M.; Ollerenshaw, J. E.; Kay, L. E., Cross-correlated relaxation enhanced 1H[bond]13C NMR spectroscopy of methyl groups in very high molecular weight proteins and protein complexes. *J Am Chem Soc* **2003,** *125* (34), 10420-8.
25. Kay, L. E.; Nicholson, A. M.; Delaglio, F.; Bax, A.; Torchia, D. A., Pulse sequences for removal of the effects of cross correlation between dipolar and chemical-shift anisotropy relaxation mechanisms on the measurement of heteronuclear T1 and T2 values in proteins. *J Magn Reson* **1992,** *97* (2), 359-375.
26. Palmer, A. G., 3rd; Skeltoni, N. J.; Chazin, W. J.; Wright, P. E.; Rance, M., Suppression of the effects of cross-correlation between dipolar and anisotropic chemical shift relaxation mechanisms in the measurement of spin-spin relaxation rates. *Mol Phys* **1991,** *75*, 699-711.